Bioactive Materials 27 (2023) 429–446

Contents lists available at ScienceDirect

Bioactive Materials

journal homepage: www.keaipublishing.com/en/journals/bioactive-materials

A new osteogenic protein isolated from *Dioscorea opposita* Thunb accelerates bone defect healing through the mTOR signaling axis

John Akrofi Kubi [a,b], Augustine Suurinobah Brah [a,b], Kenneth Man Chee Cheung [a,b], Yin Lau Lee [c,d], Kai-Fai Lee [c,d], Stephen Cho Wing Sze [e,f], Wei Qiao [g], Kelvin Wai-Kwok Yeung [a,b,*]

[a] Department of Orthopaedics and Traumatology, Li Ka Shing Faculty of Medicine, The University of Hong Kong (HKU), Hong Kong S.A.R., PR China
[b] Shenzhen Key Laboratory for Innovative Technology in Orthopaedic Trauma, HKU-Shenzhen Hospital, Shenzhen, 518053, PR China
[c] Department of Obstetrics and Gynaecology, Li Ka Shing Faculty of Medicine, HKU, 21 Sassoon Road, Hong Kong S.A.R, PR China
[d] Shenzhen Key Laboratory of Fertility Regulation, Reproductive Medicine Center, HKU- Shenzhen Hospital, Shenzhen, PR China
[e] Department of Biology, Faculty of Science, Hong Kong Baptist University, Kowloon Tong, Hong Kong S.A.R, PR China
[f] Golden Meditech Center for NeuroRegeneration Sciences, Hong Kong Baptist University, Kowloon Tong, Hong Kong S.A.R, PR China
[g] Applied Oral Sciences and Community Dental Care, Faculty of Dentistry, Hong Kong S.A.R, PR China

ARTICLE INFO

Keywords:
Dioscorea spp protein
Mesenchymal stem cells (MSCs)
Osteoblast differentiation
Bone mineral density (BMD)
Bone defect repair
mTOR signaling pathway

ABSTRACT

Delayed bone defect repairs lead to severe health and socioeconomic impacts on patients. Hence, there are increasing demands for medical interventions to promote bone defect healing. Recombinant proteins such as BMP-2 have been recognized as one of the powerful osteogenic substances that promote mesenchymal stem cells (MSCs) to osteoblast differentiation and are widely applied clinically for bone defect repairs. However, recent reports show that BMP-2 treatment has been associated with clinical adverse side effects such as ectopic bone formation, osteolysis and stimulation of inflammation. Here, we have identified one new osteogenic protein, named 'HKUOT-S2' protein, from *Dioscorea opposita* Thunb. Using the bone defect model, we have shown that the HKUOT-S2 protein can accelerate bone defect repair by activating the mTOR signaling axis of MSCs-derived osteoblasts and increasing osteoblastic biomineralization. The HKUOT-S2 protein can also modulate the transcriptomic changes of macrophages, stem cells, and osteoblasts, thereby enhancing the crosstalk between the polarized macrophages and MSCs-osteoblast differentiation to facilitate osteogenesis. Furthermore, this protein had no toxic effects *in vivo*. We have also identified HKUOT-S2 peptide sequence TKSSLPGQTK as a functional osteogenic unit that can promote osteoblast differentiation *in vitro*. The HKUOT-S2 protein with robust osteogenic activity could be a potential alternative osteoanabolic agent for promoting osteogenesis and bone defect repairs. We believe that the HKUOT-S2 protein may potentially be applied clinically as a new class of osteogenic agent for bone defect healing.

1. Introduction

The incidence of bone defects is one of the global challenges that have severe public health and socioeconomic impacts on patients [1]. The risk of bone defects increases with age-related medical conditions leading to frequent bone injuries, chronic pains, and hospitalization [2]. Bone injury stimuli trigger cellular and molecular mechanisms that modulate the sequence of events in a complex but well-orchestrated manner to progressively repair the bone defect [3]. During bone defect repairs, inflammatory activities by M1 macrophages are followed by anti-inflammatory responses mediated by M2 macrophages to stimulate MSCs to osteoblast differentiation. The macrophage-derived osteoclasts resorb the defective bone cells and matrix (bone resorption) whereas MSCs-derived osteoblasts secrete and lay down the extracellular bone matrix (bone formation) to progressively promote bone defect repair [3,4]. Molecules such as bone morphogenetic proteins (BMPs),

Peer review under responsibility of KeAi Communications Co., Ltd.
* Corresponding author.Department of Orthopaedics and Traumatology, Li Ka Shing Faculty of Medicine, The University of Hong Kong (HKU), Hong Kong S.A.R, PR China
E-mail address: wkkyeung@hku.hk (K.W.-K. Yeung).

https://doi.org/10.1016/j.bioactmat.2023.04.018
Received 21 January 2023; Received in revised form 13 April 2023; Accepted 17 April 2023

through direct activation of RUNX2, stimulate MSCs to osteoblast differentiation during bone defect repairs [5–8]. Osteogenic stimuli that modulate macrophage, MSCs, and osteoblast functions to promote osteogenesis could therefore be essential for bone defect repairs. Indeed, different studies demonstrated that controllable Mg^{2+} ion releasing-PLGA/MgO-alendronate microsphere [9], BMP-2-CPC [10], and BMB-2 protein [11] modulated macrophage, MSCs, and osteoblast activities to promote osteogenesis and bone defect healing. Although BMP-2 protein has been approved by the Food and Drug Administration (FDA) for bone defect treatments, recently, clinical adverse side effects such as ectopic bone formation, osteolysis, and stimulation of inflammation associated with BMP-2 treatments have emerged [12]. All these pieces of evidence suggest that appropriate osteogenic stimuli are required to modulate the key cellular and molecular components to enhance bone defect repairs. In recent years, cell-based therapy advancements have strongly demonstrated that the crosstalk between osteogenic cellular components plays a key role in bone defect repairs [13–15]. It has been documented that M2 macrophages enhanced mesenchymal stem cells (MSC)-osteoblast differentiation [16]. It was also reported that co-culture of M1 macrophages with MSCs enhanced osteoblast biomineralization [17]. Cell-based therapies therefore therapeutically target the crosstalk among the key cellular and molecular components for bone regeneration [15,18,19].

Furthermore, it has been reported that signaling pathways, such as mTOR signaling, are crucial in modulating bone development, functions, and tissue regeneration [20,21]. The mTOR consists of functionally distinct mTORC1 and mTORC2 protein complexes. It was reported that both mTORC1 and mTORC2 shared a common function of promoting skeletal development [22,23]. Aberration of bone-specific mTOR signaling reportedly impaired bone formation and functions [24,25]. It is therefore not surprising that mTOR signaling has been one of the targets for tissue regeneration. As mTORC1 is particularly activated by amino acids and proteins, it would be interesting to investigate whether the newly discovered HKUOT-S2 protein isolated from *Dioscorea opposita* Thunb used in this study could modulate the mTOR signaling to promote osteogenesis.

Many studies have shown that some bioactive ingredients from natural, edible foods and medicinal plants, such as *Dioscorea* spp, could be used to treat wounds and relieve pain [26]. It was reported that diosgenin and dispo85E from *Dioscorea* spp, enhanced osteogenesis in mice [27,28]. Dioscorin from *Dioscorea* spp has been reported to stimulate immunomodulatory functions in the RAW264.7 cells and mice [29]. It was also reported that an estrogenic protein, designated DOI, from *Dioscorea* spp rescued osteoporosis [30]. However, the application of *Dioscorea* spp proteins in the modulation of cellular components such as MSCs-osteoblast differentiation to enhance bone defect repairs has not been explored. Furthermore, the pharmacological activities of *Dioscorea* spp proteins in the modulation of the mTOR signaling pathway to promote osteogenesis have also not been investigated. This study therefore mainly focused on the pharmacological activities of the HKUOT-S2 protein in promoting bone defect healing and investigating the underlying osteogenic mechanism via the mTOR signaling pathway. This research demonstrated that the HKUOT-S2 protein has the potential to modulate macrophage and osteoblast functions to promote bone defect repairs. The HKUOT-S2 protein could also activate the mTOR signaling pathway to enhance osteogenesis. In summary, the newly discovered HKUOT-S2 protein, by exhibiting osteoanabolic properties, could be applied clinically as a potential osteogenic protein for bone defect repairs.

2. Materials and methods

2.1. Extraction and isolation of newly discovered HKUOT-S2 protein

The *Dioscorea opposita Thunb* tubers were bought from the wet markets in Hong Kong and authenticated by Dr. Stephen Cho Wing SZE at Hong Kong Baptist University. The extraction and isolation of the HKUOT-S2 were carried out according to the previously published protocol with some modifications [30]. With respect to the protocol modifications, the protein fraction S2 (HKUOT-S2) was isolated from the protein fraction P1 (HKUOT-P1) by size-exclusion chromatography with a loading sample volume of 100 μl and flow rate at 0.80 ml/min using the Superdex 75 increase 10/300 GL column (GE Healthcare, Sweden). Briefly, the osteogenic protein fraction D3 (HKUOT-D3) was isolated from the crude protein extracts by ion exchange chromatography using HiPrep 16/10 DEAE FF column (GE Healthcare). Next, the protein fraction P1 (HKUOT-P1) was isolated from the HKUOT-D3 by hydrophobic interaction chromatography using HiPrep 16/10 Phenyl FF columns (GE Healthcare). Finally, the protein fraction S2 (HKUOT-S2) was isolated from the HKUOT-P1 by size-exclusion Chromatography using the Superdex 75 increase 10/300 GL column.

2.2. Characterization of HKUOT-S2 protein

The HKUOT-S2 protein was subjected to electrophoresis using 15% SDS-PAGE followed by silver staining (Thermos Scientific, Hong Kong) according to the manufacturer's protocol. The HKUOT-S2 protein was processed for MALDI-MS and high-resolution liquid chromatography-tandem mass spectrometry (LC-MS/MS) analyses at the Proteomics and Metabolomics Core Facility (Pore), Centre for PanorOmic Sciences (CPOS), The University of Hong Kong (HKU). The raw MS data were processed using MaxQuant 1.6.14.0 and searched against the Dioscorea UniProt FASTA database (Jun 2020) containing 18,477 entries. Confident proteins were identified using a target-decoy approach with a reversed database and a strict false-discovery rate of 1% at peptide-spectrum matches. Targeted LC-MS/MS de novo sequences of HKUOT-S2 performed by the CPOS, HKU were matched against the NCBInr *Dioscorea* genus protein database. BlastP results with E-value <0.001, were considered significant. HKUOT-S2 N-terminal Sequencing using Edman degradation was done by Creative Proteomics Company, USA.

2.3. Animal experiment

All the animal surgical procedures were carried out strictly according to the protocol approved by the HKU Ethics Committee, Committee on the Use of Live Animals in Teaching and Research (CULATR), (CULATR 5502–20). A total of 96 C57BL/6 N male mice were used in this study. Eight to ten-week-old mice obtained from the Laboratory Animal Unit (LAU), HKU were randomly assigned into four groups namely the sham control, the 1.09 mg/kg, 2.18 mg/kg, and 4.36 mg/kg HKUOT-S2 treatment groups.

In an acute toxicity study, the mice were given subcutaneous (SC) injections of 200 μl 1X PBS for the sham controls and 200 μl HKUOT-S2 solutions for the HKUOT-S2 treatment groups thrice per week for one month. The effects of HKUOT-S2 treatments on the body weights, hematocrit, biochemistry, liver, kidney, heart, brain, lungs, and spleen histology of the mice were assessed.

In a bone defect model, 0.9 mm diameter circular-through bone defects were created on the right distal femurs, 2 mm above the epiphyseal plates. The mice were given local SC injections of 200 μl 1X PBS for the sham controls and 200 μl HKUOT-S2 solutions for the HKUOT-S2 treatment groups above the bone defect sites immediately after surgery and thrice per week for 4 weeks. The harvested bone defect regions were processed for qPCR, immunostaining, histological, and RNA-seq analyses.

2.4. Micro-computed tomography (μCT) scan analysis of the bone defects

The bone defect sites of the anesthetized mice were subjected to μCT scanning immediately after the surgery using the Skyscan (Bruker) followed by weekly μCT scans for 1 month. The X-ray images obtained from the μCT scans were reconstructed into 2D images using the NRecon

software (Skyscan, Bruker). The CTvox and CTAn software was used to evaluate the bone defect repairs.

2.5. Fluorochrome labeling

The mice were administered an intraperitoneal injection of 10 mg/kg Calcein green (Sigma-Aldrich) on day 19 and post-surgery and 90 mg/kg xylenol orange (Sigma-Aldrich) three days before euthanasia. The harvested undecalcified femurs were fixed in 10% neutral buffered formalin (10% NBF) and embedded in methyl methacrylate (MMA) (Sigma-Aldrich). The inverted confocal fluorescence microscope, Carl Zeisis (LSM900) equipped with the ZEISS (ZEN 3.4, blue edition) software was used to acquire and quantify the fluorochrome intensities of the 50 μm section of the bone tissues at the bone defect sites.

2.6. Histological analyses of the bone defect sites

The harvested bone defect sites were fixed in 10% NBF, decalcified in 0.5 M ethylenediaminetetraacetic acid (EDTA) (Sigma-Aldrich), dehydrated, and embedded in paraffin. The decalcified bone defect regions were processed for Masson's trichrome staining (Sigma-Aldrich) and hematoxylin and eosin (H &E) staining whereas the undecalcified bone defect regions were processed for Giemsa staining (Merck).

2.7. TRACP and ALP staining of paraffin-embedded bone sections

TRACP and ALP staining was performed on 4 μm bone sections using TRACP & TRAP double stain kit (Takara) following the manufacturer's guidelines. The TRACP & TRAP double stained bone tissues on the slides were viewed under Eclipse 80i compound fluorescence microscope.

2.8. Transmission electron microscopy (TEM)

2 mm of the decalcified bone defect sites were processed for TEM analysis at the Electron Microscopy Unit, HKU. The Philips CM100 TEM was used to acquire detailed images of the bone tissue sections for qualitative cellular and intracellular ultrastructural analyses.

2.9. Enzyme-linked immunosorbent assay (ELISA)

The HKUOT-S2-induced ALP and OCN levels in the bone defect sites were evaluated by mouse BALP (CUSABIO) and mouse osteocalcin (Novus Biological) ELISA kits according to the manufacturer's instructions. The total proteins were used to normalize the BALP and OCN levels.

2.10. Immunofluorescence staining

Immunofluorescence staining for ALP, OCN, and RUNX2 was performed on the bone defect sites according to the published standard protocol [31].

2.11. rRNA-depleted RNA-sequencing

High-quality, total RNAs from the bone defect region were double extracted using RNAiso plus reagent (Takara) and PureLink™ RNA Mini Kit (Thermo Scientific, Hong Kong) according to the manufacturer's instructions. The RNA samples were processed for rRNA-depleted RNA sequencing (RNA-seq) at CPOS Genomics Core, HKU. Transcriptome pair-wise bioinformatics analysis was used to generate HKUOT-S2-induced differentially expressed genes and transcripts in the defective bones with FDR<0.05. The HKUOT-S2-induced gene-enriched KEGG pathways and GO terms were evaluated using the Partek genomic suite software. The heatmaps were plotted with gplots using z-scores.

2.12. In vitro cell culture

The mouse M0 macrophage, RAW264.7 cells (Cat# TIB-74), and human pro-monocyte, U937 cells (Cat# CRL-1593.2) were purchased from the American Type Culture Collection (ATCC). The human turbinate mesenchymal stromal cell line (hMSCs), harvested by Kwon et al. [32], was also used in this study. The RAW264.7 cells were cultured in DMEM high glucose medium supplemented with 3.72 mg/ml $NaHCO_3$, 5.685 mg/ml, HEPES, 10% heat activated fetal bovine serum (FBS), 2 mM L-glutamine, 0.25 μg/ml amphotericin B, and 100U/ml penicillin-streptomycin (P/S). The U-937 cells were cultured and maintained in RMPI medium 1640 (1X) (Thermo Fisher Scientific) supplemented with 10% FBS and 100U/ml P/S. Both the RAW264.7 and U-937 cells were passaged every 3 days. The hMSCs were cultured for 4–5 days in DMEM low glucose medium (Thermo Fisher Scientific) supplemented with 10% FBS and 100U/ml P/S. The cell culture medium was replaced every 3 days and the cells were passaged at 80% confluence. All the cells were kept in the humidified incubators at 37 °C and 5% CO_2.

2.13. HKUOT-S2 protein fluorescent labeling and interaction with cells

The HKUOT-S2 protein was covalently labeled with Alexa Fluor 568 fluorescence signal using the Alexa Fluor 568 Conjugation Kit (Fast)-Lightning-Link (Abcam, ab269821) according to the manufacturer's protocol. The Alexa Fluor 568 conjugated HKUOT-S2 protein was used to treat hMSCs and U-937 cells for 2 h. The interaction between the HKUOT-S2 protein and the hMSCs or U-937 cells was evaluated using confocal fluorescence microscopy and flow cytometry analysis.

2.14. Effects of HKUOT-S2 on macrophage polarizations and cytokine array analysis

The RAW264.7 and U937 cells were seeded at 2×10^4 cells/well and cultured for 24 h. The U937 cells were differentiated into M0 macrophages with 20 ng/ml Phorbol 12-myristate 13-acetate (PMA) (Sigma-Aldrich). Both the RAW264.7 and U937 cells were either polarized into M1 or M2 macrophage using 100 ng/ml lipopolysaccharide (LPS) (Sigma-Aldrich) or 20 ng/ml human IL-4 (R&D System) respectively, with or without 0.1 μg/ml HKUOT-S2 protein. The non-polarized cells were used as controls. The U937 cell-derived M1 and M2 macrophage condition media (CM) were collected for cytokine array analysis using the Mouse XL Cytokine Array Kit (R&D Systems) according to the manufacturer's protocol.

2.15. Flow cytometry analysis of HKUOT-S2 treated primary M0-derived macrophages

Primary bone marrow macrophages were harvested from the 8 weeks old mice [33]. The primary M0 macrophages were polarized into M1 or M2 macrophages with or without HKUOT-S2 protein. Singleton cell suspensions were processed and co-stained with fluorescent labeled CD206, and MGL-1 antibodies (Cell Signaling) for flow cytometry analysis using an Agilent NovoCyte Quanteon analyzer.

2.16. Effects of HKUOT-S2 treatment on osteoblast biomineralization

The hMSCs seeded were at 2.5×10^4 cells/well, treated with osteogenic medium containing 100 nM dexamethasone, 10 mM β-glycerophosphate, 0.28 mM ascorbic acid (Sigma-Aldrich), and macrophage CM in 1:1 ratio with or without HKUOT-S2 protein for 10 days with media replacement every 3 days. ALP activity assay was performed on the differentiated osteoblasts with or without BMP-2 or HKUOT-S2 treatments using the 1-Step NBT/BCIP kit according to the manufacturer's instructions (Thermo Scientific). The cells also were fixed with 4% paraformaldehyde and stained with Alizarin Red S (ARS) (Sigma-

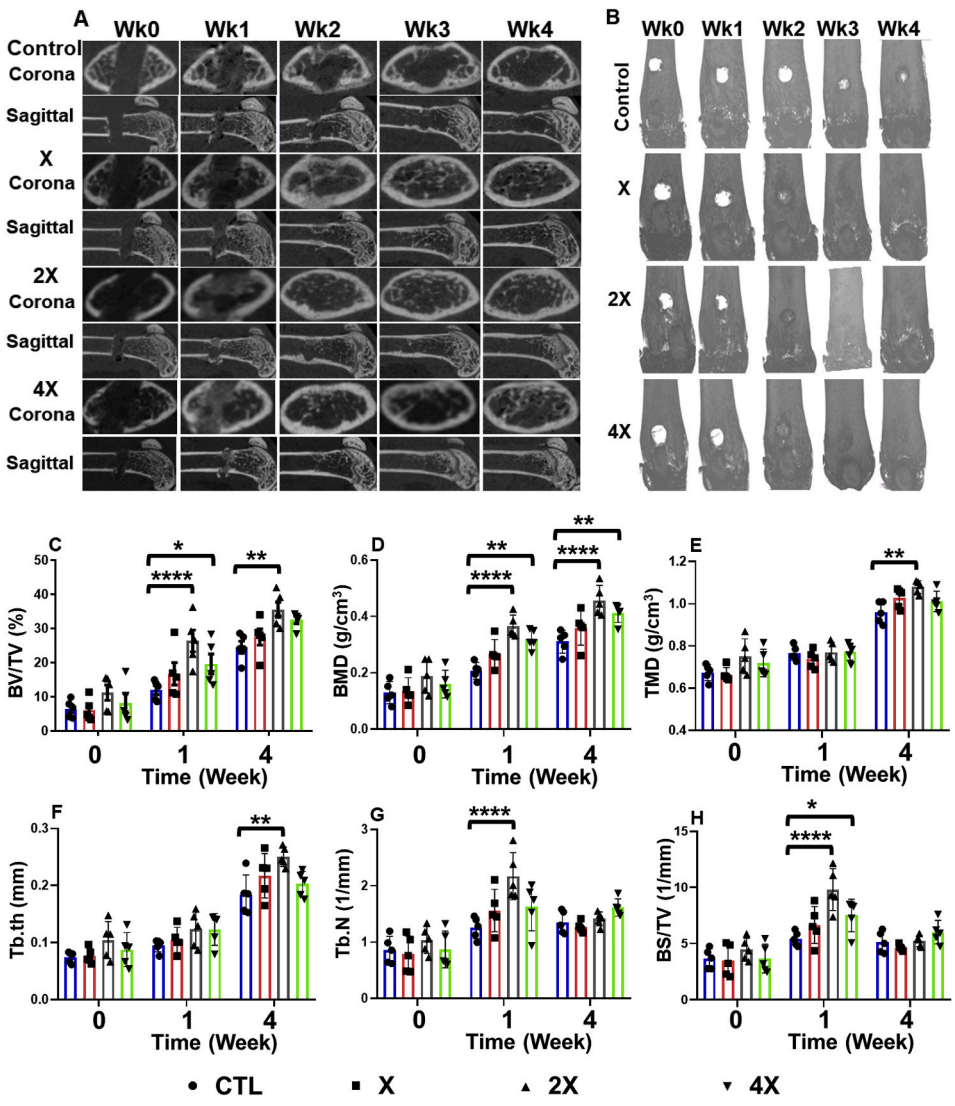

Fig. 1. HKUOT-S2 significantly enhanced bone defect repairs *in vivo*. A) Representative μCT scans of the bone defect sites of the sham control and HKUOT-S2 treatment groups. B) 3D reconstructed images of the μCT scans of the bone defect sites of the sham control and HKUOT-S2 treatment groups. C–H) μCT analysis of BV/TV, BMD, TMD, Tb.th, Tb. N, and BS/TV ratio showing bone defect healing process. The values were shown as mean ± SEM, n = 5. X, 2X, and 4X = 1.09 mg/kg, 2.18 mg/kg, and 4.36 mg/kg HKUOT-S2 treatments respectively. *p < 0.05, **p < 0.01, ***p < 0.001 and ****p < 0.0001.

Aldrich). The amount of biomineralization was quantified at 405 nm using the microplate reader.

2.17. Effects of HKUOT-S2 treatment on mTOR signaling during osteoblast differentiation

XL388 is a potent mTOR inhibitor. To investigate the effect of HKUOT-S2 protein on the mTOR signaling during osteogenesis, the differentiating hMSCs were treated with 125–500 nM XL388 (Sigma-Aldrich) or 0.1 μg/ml HKUOT-S2 protein for 7 days, with medium refreshments every 3 days, during the hMSCs-osteoblast differentiation.

2.18. Quantitative real-time polymerase chain reaction (qPCR) analysis

Total RNAs were extracted from the cell lines and bone tissues using RNAiso plus reagent (Takara). The RNAs were reverse transcribed into complementary DNA (cDNA) using the PrimeScript™ RT reagent Kit (Takara). Specific primer pairs (Table S6 and Table S7) were used to determine the mRNA levels using the QuantStudio 5 real-time PCR system (Thermo Scientific). The gene expression fold changes were calculated by the $2^{-\Delta\Delta Ct}$ method after *GAPDH* normalization.

2.19. Western blot analysis

The cells and bone tissues were lysed with RIPA buffer (Thermo Scientific). The total proteins were measured spectrophotometrically using Pierce Coomassie Plus (Bradford) Protein Assay kit (Thermo Scientific). Normalized protein samples were separated by SDS-PAGE electrophoresis and transferred to PVDF membranes for 2hrs in a cold transfer buffer. The membranes were blocked with 10 ml of PBST containing 5% BSA (GoldBio) for 30 min, incubated with primary antibodies (Table S8) at 4 °C overnight, secondary antibodies (Table S8) for 2hrs at room temperature and Pierce™ ECL Western Blotting Substrate (Thermo Scientific). The targeted protein band intensities were analyzed using GE Amersham Imager AI680.

2.20. Statistical analysis

A Student's t-test or One-way ANOVA followed by Turkey's test post-hoc comparisons for normal distribution and Kruskal-Wallis post-hoc comparisons for non-parametric tests were used for statistical analyses using GraphPad Prism 8.0 (GraphPad Software, CA, USA). The values were shown as mean ± SEM. *p < 0.05 was considered significant.

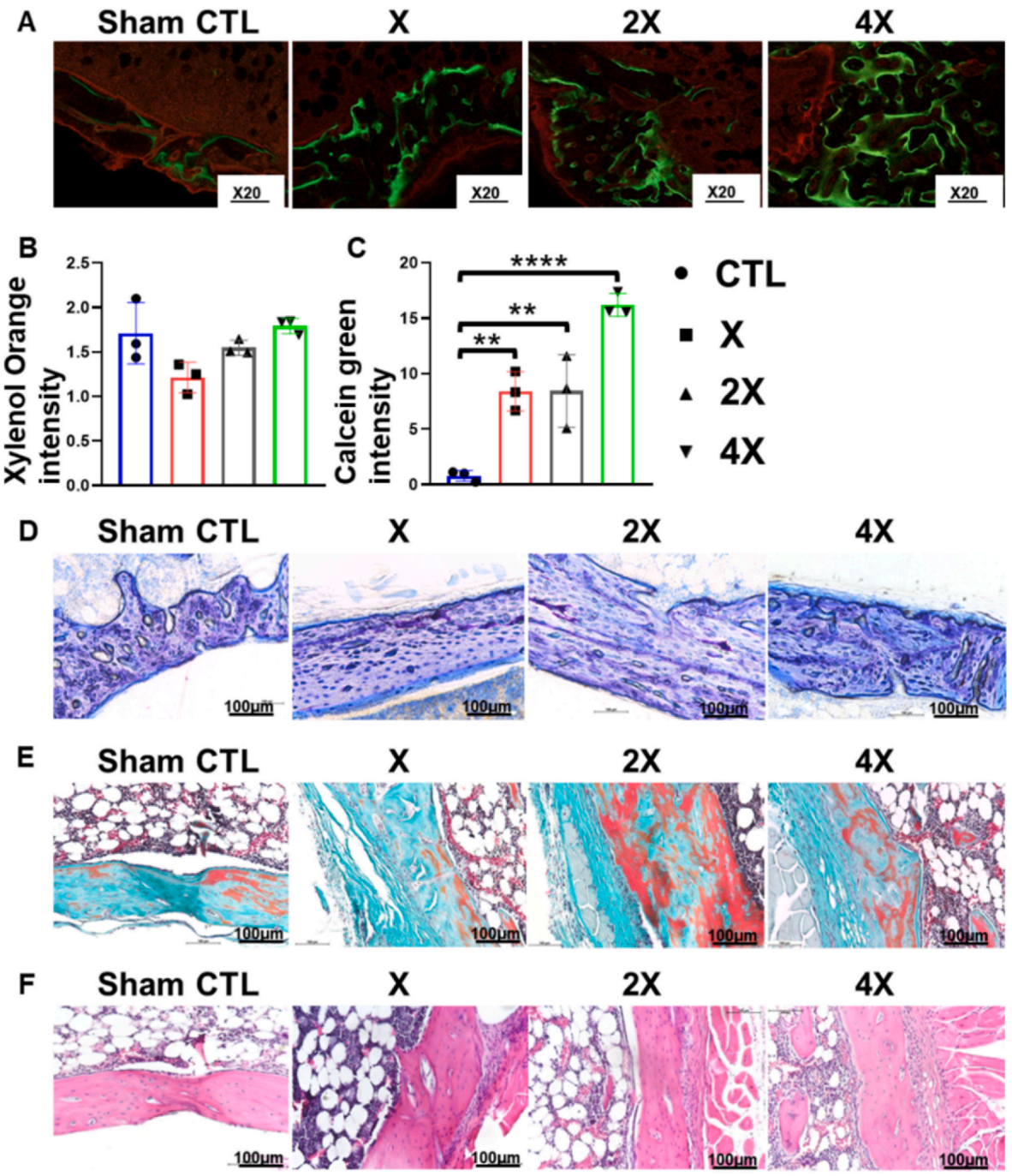

Fig. 2. HKUOT-S2 enhanced new bone formation. A) Representative images of fluorochrome labeling (red for xylenol orange and green for Calcein green) for new bone formation at bone defect sites of the sham control and HKUOT-S2 treatment groups. B) Quantification of xylenol orange fluorescence intensity at bone defect sites of the sham control and HKUOT-S2 treatment groups. C) Quantification of calcein green fluorescence intensity at bone defect sites of the sham control and HKUOT-S2 treatment groups. D) Representative images of Giemsa staining of bone defect sites of the sham control and HKUOT-S2 treatment groups. E) Representative images of Masson-Goldner trichrome staining of bone defect sites of the sham control and HKUOT-S2 treatment groups. F) Representative images of H&E staining of bone defect sites of the sham control and HKUOT-S2 treatment groups. The values were shown as mean ± SEM. n = 4, X, 2X, and 4X = 1.09 mg/kg, 2.18 mg/kg, and 4.36 mg/kg HKUOT-S2 treatments respectively. **$p < 0.01$, ****$p < 0.0001$.

3. Results and discussions

3.1. HKUOT-S2 protein isolation and characterization

The *Dioscorea* spp tubers are among the most globally consumed crops due to their high nutritional and medicinal values [34,35]. They are general high-energy packed carbohydrate foods that contained only about 1.5% total protein [35,36]. Dioscorin (200 kDa) forms the major protein component of the limited bioactive *Dioscorea* spp proteins discovered [37]. Also, the majority of the discovered *Dioscorea* spp proteins (Dioscorin (200 kDa) and diosgenin (414.6 kDa)) have high molecular weights. Data on the lower molecular weight osteogenic *Dioscorea* spp proteins are very scanty. In this study, the lower molecular weight HKUOT-S2 protein (32 kDa) was successfully isolated with homogeneity from the protein fraction HKUOT-P1 (Figs. S1A–F). Phytochemical analysis indicated that the HKUOT-S2 is a protein (Table S1)

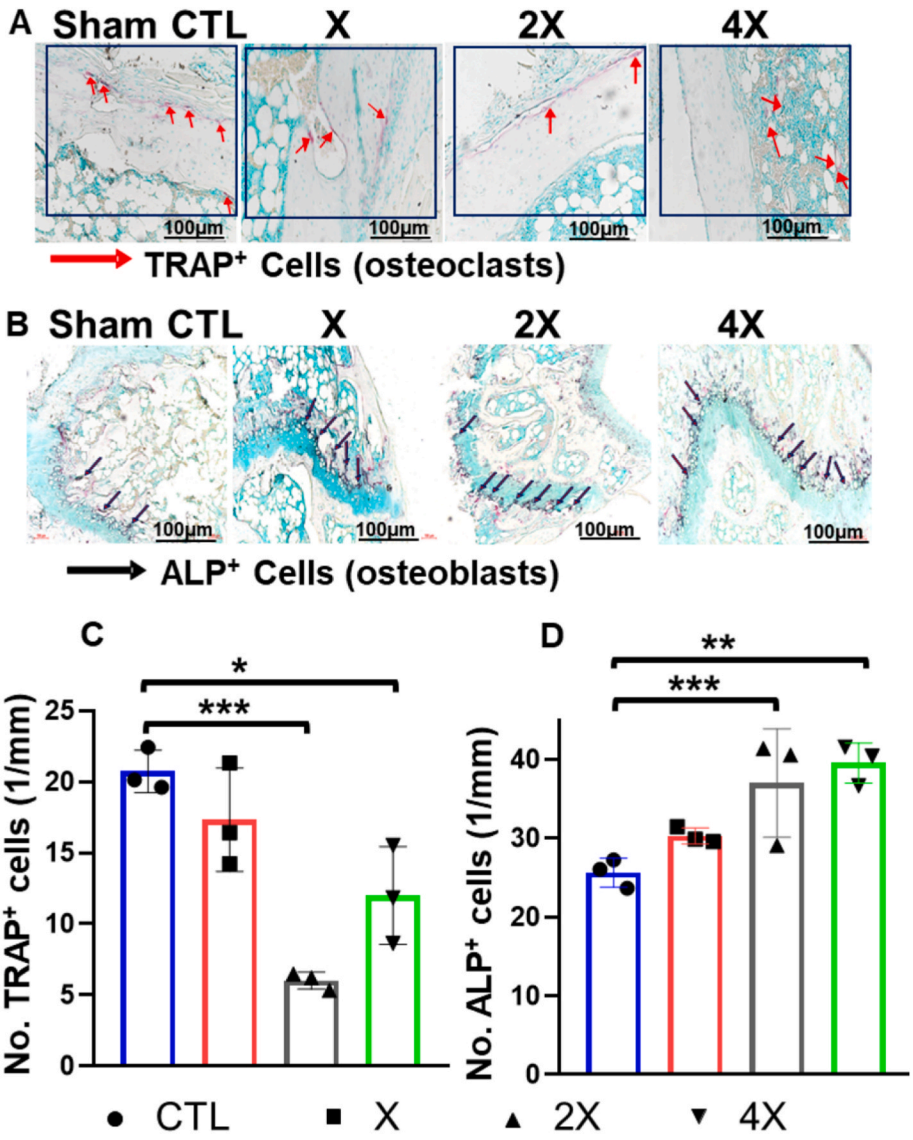

Fig. 3. HKUOT-S2 enhanced osteoblast activity *in vivo*. A) Representative images of TRACP staining showing the $TRAP^+$ cells at bone defect sites of the sham control and HKUOT-S2 treatment groups. B) Representative images of ALP staining showing the ALP^+ cells at bone defect sites of the sham control and HKUOT-S2 treatment groups. C) Quantification of $TRAP^+$ cells at bone defect sites of the sham control and HKUOT-S2 treatment groups. D) Quantification of ALP^+ cells at bone defect region of the sham control and HKUOT-S2 treatment groups. The values were shown as mean ± SEM. n = 4, X, 2X, and 4X = 1.09 mg/kg, 2.18 mg/kg, and 4.36 mg/kg HKUOT-S2 treatments respectively. *p < 0.05, **p < 0.01, ***p < 0.001 and ****p < 0.0001.

[38]. The HKUOT-S2 protein constituted about 2.5% of the total *Dioscorea opposita* Thunb crude protein extracted. The molecular mass of the HKUOT-S2 protein as determined by SEC column calibration [27, 39], silver staining, and mass spectrometry was 32 kDa (Fig. 1E and F; Table S2). High-resolution liquid chromatography-tandem mass spectrometry (LC-MS/MS) analysis revealed the HKUOT-S2 peptide sequences, and de novo peptide sequences (Fig. S1G, Table S3, Table S4). The unique HKUOT-S2 peptide sequences did not match with any known proteins of the entire plant kingdom, including that of the *Dioscorea* spp proteins, downloaded from UniProt and NCBInr *Dioscorea* genus protein database. NCBI BlastP analysis of the HKUOT-S2 peptide sequences had an E-value <0.001 which implied that the HKUOT-S2 is potentially novel. N-terminal Sequencing of HKUOT-S2 revealed the HKUOT-S2 N-terminal sequence as **IKITTYRQ** corresponding to the three-letter sequence **Ile-Lys-Ile-Thr-Thr-Tyr-Arg-Gln**. The HKUOT-S2 protein and peptide sequences have been approved by The University of Hong Kong (HKU) Patent Committee, Technology Transfer Office (HKU TTO Ref: IP01212) as a novel protein followed by the US Patent Application (application number 63/371,229). This research has therefore contributed to scientific knowledge by adding a new osteogenic protein to the few list of already known *Dioscorea* spp proteins.

3.2. HKUOT-S2 protein treatments had no toxic effects

The discovery of new compounds is usually accompanied by safety concerns within the context of the intended potential clinical applications. Safety concerns have been raised in the usage of most classical anti-osteoporotic drugs that augment bone integrity [40]. A toxicity study was therefore carried out to ensure that the HKUOT-S2 protein was safe for downstream *in vivo* applications. To determine the anti-hemolytic property of HKUOT-S2 protein, mice red blood cells (RBCs) were subjected to HKUOT-S2 treatments, and the results were compared with that of the different drugs such as diclofenac, melittin, and piscidin. Diclofenac (non-hemolytic) is a well-known nonsteroid anti-inflammatory drug (NSAID) for pain relief [41]. Melittin, an anti-microbial peptide that constitutes the main pain-inducing agent of bee venom, reportedly caused hemolysis in mice [42]. Piscidin, an anti-microbial peptide from fish, reportedly did not induce significant hemolysis of human RBCs [43]. The hemolytic test showed that HKUOT-S2 treatments did not induce any hemolysis when compared with the positive controls (1X triton-X-100 and melittin) for hemolysis (Fig. S2A). The hemolytic activity of hypotonic solution has been well documented [44]. To investigate the degree of hemolytic inhibition effects of HKUOT-S2 protein, a hypotonic solution-induced hemolysis test was performed by treating mouse RBCs with different concentrations of

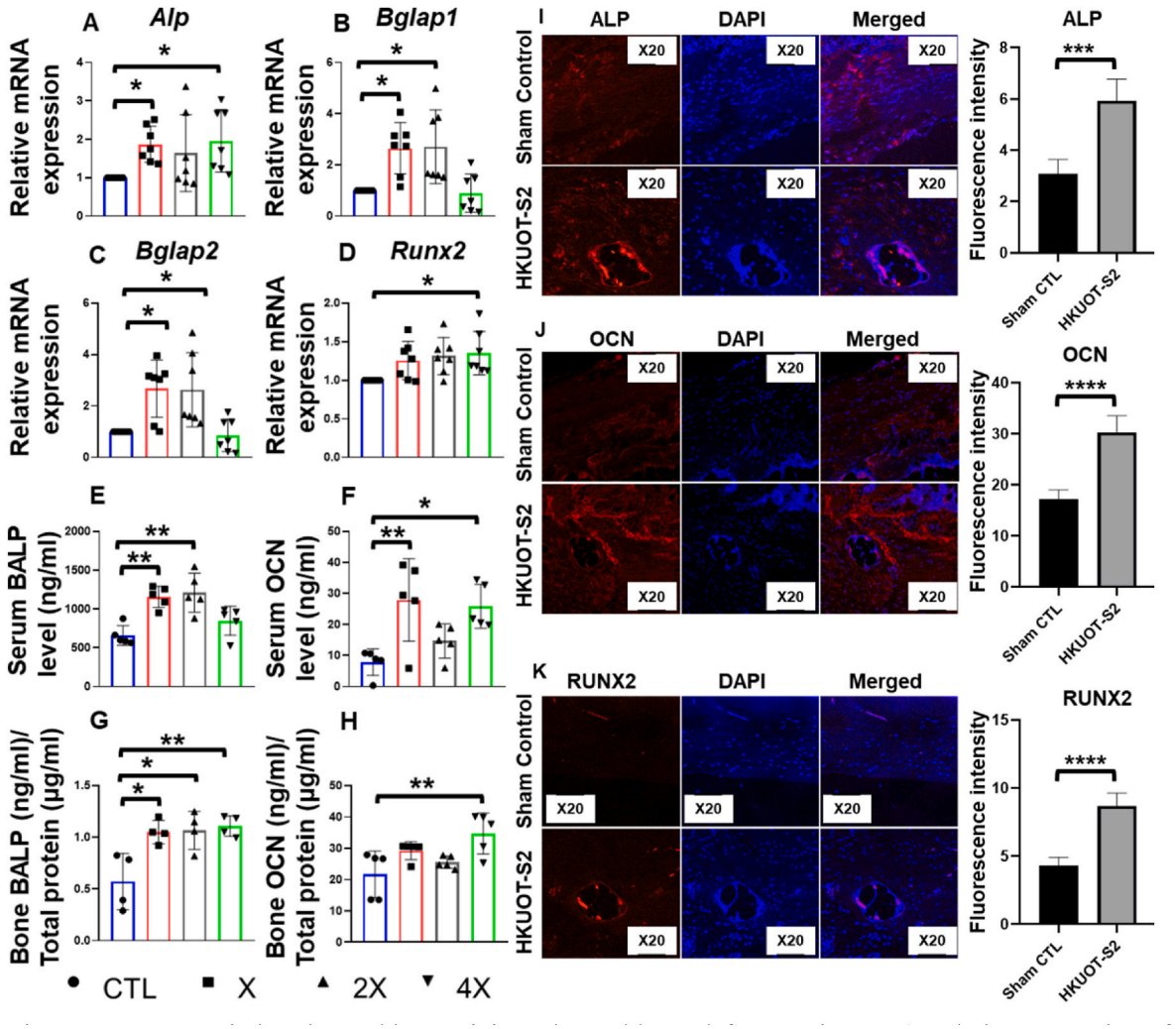

Fig. 4. HKUOT-S2-induced osteoblast activity enhanced bone defect repairs. A-D) Relative expression of osteogenic markers, *Alp, Bglap1, Bglap1,* and *Runx2* expressions in the bone defect sites of the sham control and HKUOT-S2 treatment groups. E-H) ELISA analysis of BALP and OCN proteins levels in both serum and bone lysates from the bone defect site of the sham control and HKUOT-S2 treatment groups. I–K) Representative immunofluorescent and measurement of ALP, OCN, and RUNX2 expression at the bone defect sites of the sham control and HKUOT-S2 treatment groups. The values were shown as mean ± SEM. X, 2X, and 4X = 1.09 mg/kg, 2.18 mg/kg, and 4.36 mg/kg HKUOT-S2 treatments respectively. *p < 0.05, **p < 0.01.

NaCl solution in the presence of HKUOT-S2 protein, diclofenac, piscidin or BSA. The results showed that 100 μg/ml HKUOT-S2 protein treatment partially inhibited hypotonic solution (0.45% NaCl)-induced hemolysis when compared to the diclofenac, piscidin or BSA treatments (Figs. S2B and C). Taken together, the hemolytic test results demonstrated that HKUOT-S2 protein was not only nonhemolytic but also partially protected the RBCs against hypotonic solution-induced hemolysis. Furthermore, an acute toxicity study was performed to evaluate the potential toxic effect of HKUOT-S2 treatments in mice. Giemsa staining of the blood smears showed that the blood cells in both sham control and the HKUOT-S2 protein treatment groups were well conserved indicating that HKUOT-S2 protein treatments had no toxic effects on the blood cell elements (Fig. S2D). HKUOT-S2 protein treatments also had no significant toxic effects on the body weights, hematocrits, and clinical biochemistry of the mice (Figs. S3A–H). H&E staining results showed that HKUOT-S2 treatment did not elicit any toxic effects on the histology of the liver, kidney, heart, brain, lung, and spleen of the mice (Fig. S4A). qPCR analysis showed that HKUOT-S2 treatments had no significant toxic effects on liver and kidney function gene expressions (Figs. S4B–I). Generally, bioactive compounds from natural sources are considered relatively safer in terms of clinical applications when compared with synthetic ones [45]. As the HKUOT-S2 protein is isolated from a natural, edible food source, it was unsurprised that the therapeutic doses of the HKUOT-S2 protein elicited no toxic effect *in vivo*. All the toxicity study's results demonstrated that the therapeutic doses of HKUOT-S2 protein treatments used in this research were safe for downstream *in vivo* application.

3.3. HKUOT-S2 significantly enhanced bone defect repairs in vivo

Bone defect incidence is common among the aging human population. Without appropriate medical interventions, bone defects heal at slower rates, and become prone to infections [4]. In this study, the biological functions of the HKUOT-S2 protein were investigated in the bone defect model to establish a solid foundation for its potential clinical applications. Micro-computed tomography (μCT) scan analysis showed that HKUOT-S2 protein promoted osteogenesis and bone defect healing by significantly increasing bone volume (BV/TV), bone mineral density (BMD), tissue mineral density (TMD), trabecular thickness (Tb.th), trabecular number (Tb. N) and bone surface area to tissue volume (BS/TV) ratio (Fig. 1A–H). The HKUOT-S2 protein could therefore be applicable for treating bone defects, thereby preventing delayed bone defect healing, reducing the risks of infections, and shortening the hospitalization periods of patients.

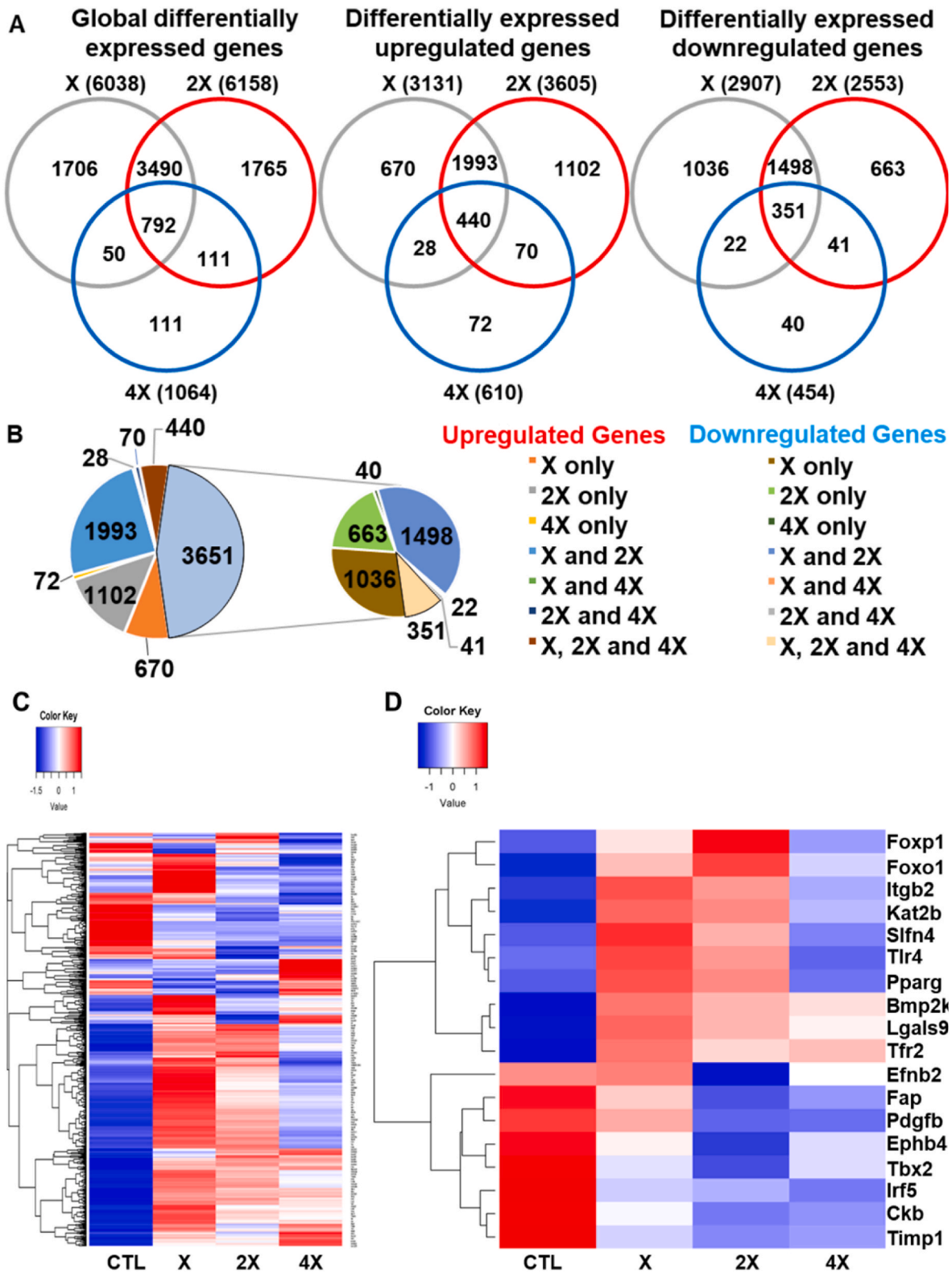

Fig. 5. HKUOT-S2 treatments induced transcriptomic changes to promote bone defect healing. A) Venn diagrams of HKUOT-S2-induced differentially expressed genes (*left*), differentially upregulated (*middle*), and downregulated genes (*right*). B) Pie chart showing the distribution of HKUOT-S2-induced differentially expressed genes. C) Heatmap of general differentially expressed genes induced by HKUOT-S2 protein treatments. D) Heatmap of HKUOT-S2-induced most common differentially expressed genes.

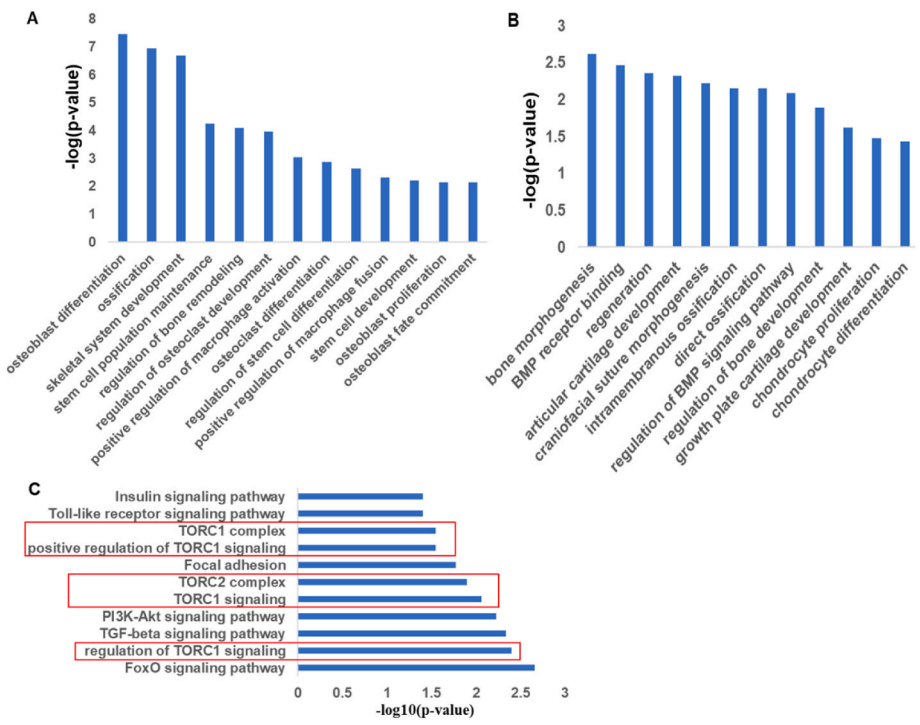

Fig. 6. HKUOT-S2 treatments modulated cellular components and mTOR signaling pathway to promote bone defect healing. A) Both X and 2X HKUOT-S2 enriched GO terms are associated with macrophages, stem cells, and osteoblasts functions. B) Both X and 2X HKUOT-S2 treatment enriched GO terms associated with bone formation. C) Both X and 2X HKUOT-S2 enriched the mTOR signaling pathway. The values were shown as mean ± SEM, n = 3. X, 2X, and 4X = 1.09 mg/kg, 2.18 mg/kg, and 4.36 mg/kg (4X) HKUOT-S2 treatments respectively. *p < 0.05 and **p < 0.01.

3.4. Fluorochrome labelling and histological analysis of HKUOT-2-induced bone defect repairs

Osteoblasts are architects of new bone formation and are therefore the therapeutic targets of most anabolic agents, such as teriparatide, which augment bone mineralization and accelerate bone defect healing [46,47]. Plant-based anabolic ursolic acid reportedly increased osteoblast activity to enhance new bone formation [48]. In this study, the effects of the HKUOT-S2 treatments on osteoblast activity to facilitate new bone formation was evaluated by *in vivo* fluorochrome labeling and histological analyses. HKUOT-S2 treatments significantly increased new bone formation (higher fluorescence intensities of the Calcein G) at the bone defect sites (Fig. 2A, C). The Giemsa staining results showed that the collagen fibers (pink in color) at the bone defect sites were well organized in the HKUOT-S2-induced bone defect healing (Fig. 2D). The Masson-Goldner trichrome staining showed that HKUOT-S2 treatments induced more bone mineralization with red staining (mature bone matrix) compared to the sham control (Fig. 2E). The H&E staining revealed that the bone defects were repaired in the HKUOT-S2 treatment groups (Fig. 2F). Taken together, the results showed that HKUOT-S2 treatment could increase osteoblast activity to promote bone defect repairs.

3.5. HKUOT-2 modulated osteoblast and osteoclast activities to enhance bone defect repairs

TRAP and ALP immunohistochemistry (IHC) staining results revealed that the 2.18 mg/kg HKUOT-S2 treatment significantly decreased osteoclast activities ($TRAP^+$ cells, red arrows) but increased osteoblast activities (ALP^+ cells, black arrows) to promote bone defect healing (Fig. 3A–D). Transmission electron microscope (TEM) analysis of the bone defects sites revealed that there were more osteoblast-like cells with euchromatic nuclei and fewer osteoclast-like cells with heterochromatic nuclei found in the HKUOT-S2 protein treatment groups when compared with the sham control (Figs. S5A–C). The results indicated that HKUOT-S2 protein treatments might have increased osteoblast activities to promote bone defect repairs. The osteoanabolic activity of the HKUOT-S2 protein is supported by the reports that osteoanabolic agents such as teriparatide, human parathyroid hormone (PTH) analogues, PTH-related peptide (PTHrp) and plant-based anabolic ursolic acid also modulated osteoblast activities to augment bone mineralization and accelerate bone defect healing [46–49].

3.6. HKUOT-S2 treatment increased osteogenic genes and protein expressions

To demonstrate that the HKUOT-S2 protein treatment indeed enhanced osteoblast activities to promote bone defect repairs, the bone tissues from the bone defect sites were subjected to osteogenic gene expression, immunoassay, and immunofluorescent staining analyses. The qPCR results showed that HKUOT-S2 treatments significantly increased osteoblast gene expressions, *Alp, Bglap1*, *Bglap2,* and *Runx2,* in the defective bones (Fig. 4A–D). Both *Bglap1* and *Bglap2* encode for osteocalcin (OCN) protein [50]. Enzyme-linked immunosorbent assay (ELISA) analysis using the bone-specific ALP (BALP) and osteocalcin (OCN) ELISA kits showed that HKUOT-S2 treatments significantly increased BALP and OCN levels in both the sera and bone defect lysates (Fig. 4E–H). Immunofluorescent staining revealed that HKUOT-S2 protein treatment significantly increased ALP, OCN, and RUNX2 protein expression at the bone defect regions when compared with that of the sham control (Fig. 4I–K). The HKUOT-S2 protein-induced osteoblast differentiation markers, *Alp, Runx2*, and *Bglap*, confirmed the osteoanabolic activity of the HKUOT-S2 protein in bone defect healing.

3.7. Transcriptomic analysis of HKUOT-S2-induced bone defect healing

To investigate whether HKUOT-S2 protein treatments induced differential transcriptomic changes that might have contributed to the enhanced bone defect repairs, total RNAs isolated from the bone defect regions of the sham control and HKUOT-S2 treatment groups were processed for ribosomal RNA (rRNA)-depleted RNA sequencing (RNA-seq). It is well known that rRNA constitutes about 90% of the total RNA and could interfere with the correct acquisition and interpretation of the RNA-seq data [51].To acquire the most relevant RNA-seq data, the rRNA was depleted in the RNA samples of the bone defect tissues prior to the RNA-seq.

Analysis of the transcriptomic data revealed that HKUOT-S2

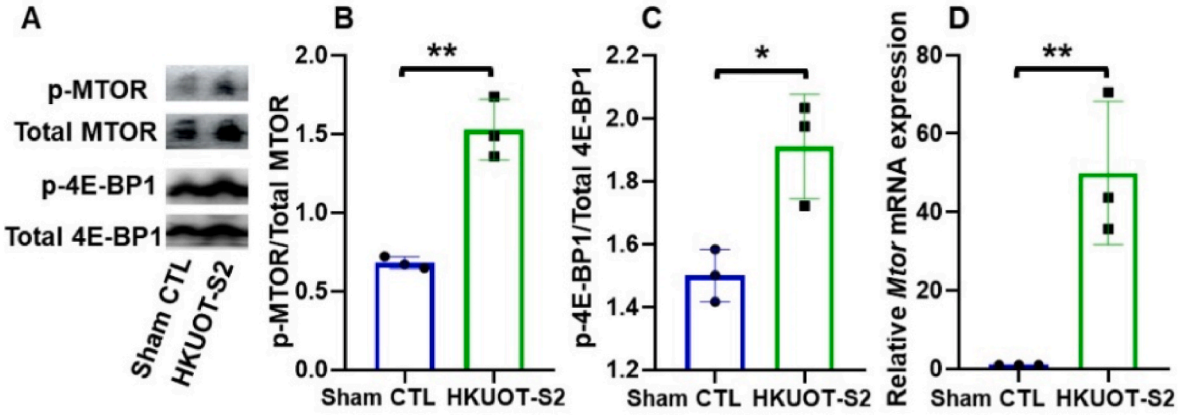

Fig. 7. HKUOT-S2 treatments activated the mTOR signaling to promote bone defect healing *in vivo*.
A-C) Representative Western blot images and corresponding quantification of p-mTOR/total mTOR protein and p-4E-BP1/total 4E-BP1 protein in the bone defect sites of the sham control and HKUOT-S2 treatment groups. D) Relative *Mtor* mRNA expression in the bone defect sites of the sham control and HKUOT-S2 treatment groups. The values were shown as mean ± SEM, n = 3. *p < 0.05, **p < 0.01.

treatments induced differentially expressed genes and transcripts in the bone defect tissues. Filtering of the differentially expressed genes and transcripts with FDR <0.05 showed that 1.09 (X), 2.18 (2X), and 4.36 (4X) mg/kg HKUOT-S2 treatments induced 6038, 6158, and 1064 genes, 9477, 9974 and 2871 transcripts respectively (Table S5). Among the differentially expressed genes, 792 genes were commonly shared by all three doses, 3490 genes were common to only X and 2X doses, 111 genes were only found in both 2X and 4X doses, 50 genes were common to only X and 4X doses of HKUOT-S2 treatments (Fig. 5A (*left*)). Among the differentially expressed genes, 440 upregulated and 351 downregulated genes were found to be common to all three doses of HKUOT-S2 treatments (Fig. 5A (*middle and right*)). 54% and 46% of the differentially expressed genes were upregulated and downregulated respectively (Fig. 5B, Table S6). Heatmaps of the general and most common differentially expressed genes showed the transcriptional distances between the sham control and HKUOT-S2 treatment groups (Fig. 5C and D). The results showed that HKUOT-S2 treatment modulated transcriptomic changes to promote bone defect repairs.

3.8. *HKUOT-S2 significantly enriches cellular components and the mTOR signaling pathway*

Macrophages, MSCs, osteoclasts, and osteoblasts coordinate to facilitate bone defect repairs [52,53]. Functional transcriptome data

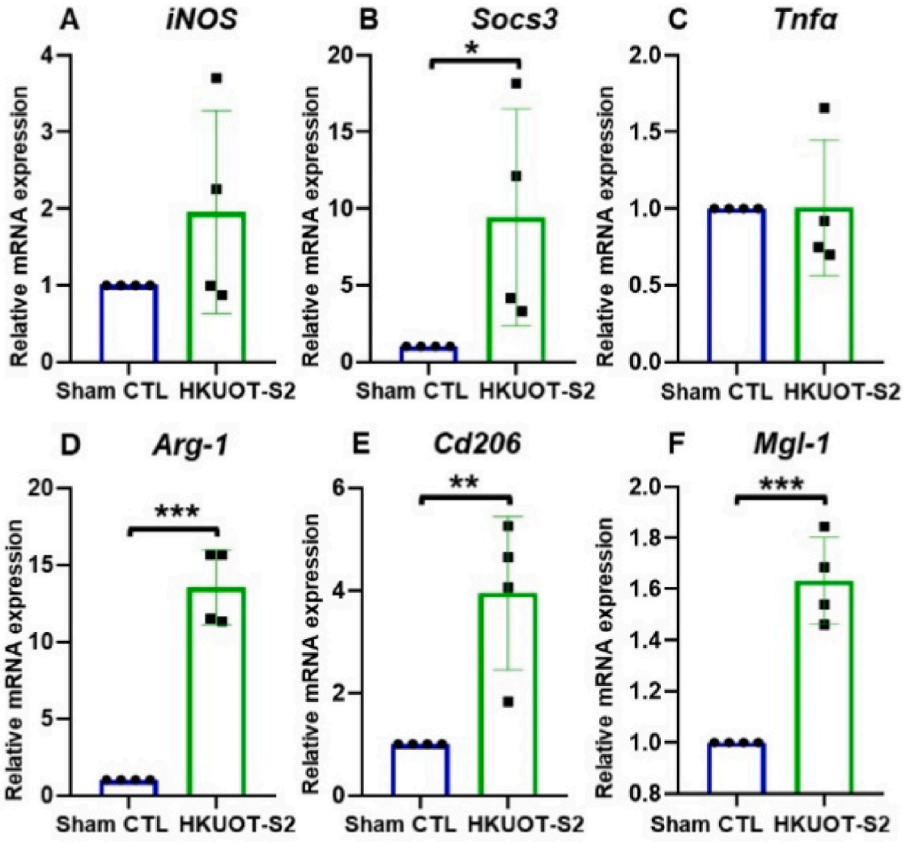

Fig. 8. HKUOT-S2 treatment significantly enhanced anti-inflammatory activity *in vivo* to promote bone defect repairs. A-C) Relative M1 macrophage gene expressions (*iNos*, *Socs3,* and *Tnfα*) in the bone defect sites of the sham control and HKUOT-S2 treatment groups. D-F) Relative M2 macrophage gene expressions (*Arg-1*, *Cd206,* and *Mgl-1*) in the bone defect sites of the sham control and HKUOT-S2 treatment groups. The values were shown as mean ± SEM, n = 4. *p < 0.05, **p < 0.01, ***p < 0.001 and ****p < 0.0001.

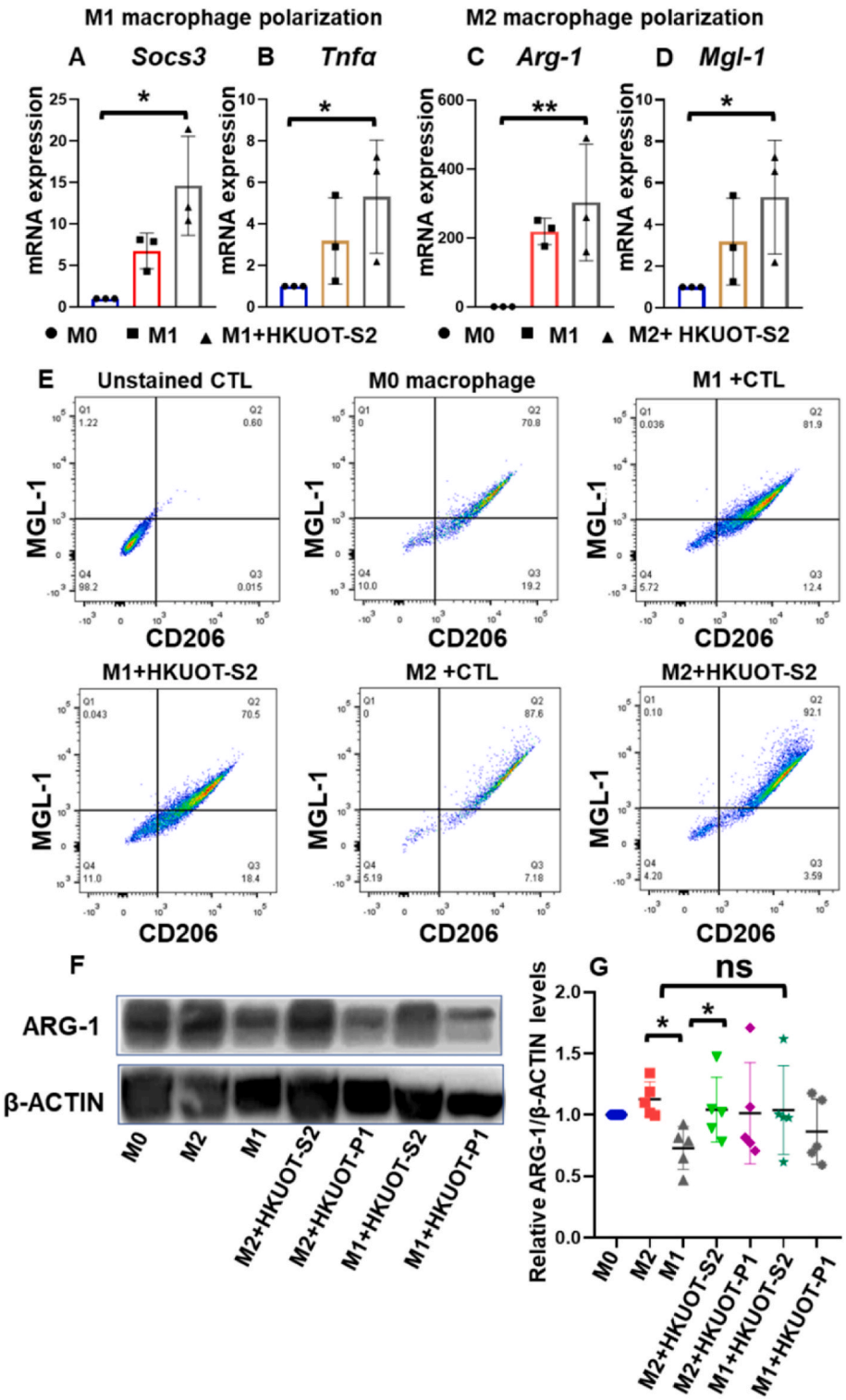

Fig. 9. HKUOT-S protein modulated macrophage polarization. A, B) Relative expression of *Socs3* and *Tnfα* in the control and HKUOT-S2 treated M1 macrophages derived from RAW267.4 cells. C, D) Relative expression of *Arg-1* and *Mgl-1* in the control and HKUOT-S2 treated M2 macrophages derived from RAW267.4 cells. E) Flow cytometry analysis showing expression of CD206 and MGL-1 double-positive control and HKUOT-S2 treated M1 and M2 macrophages derived from the primary bone marrow macrophage (M0 macrophage). F, G) Representative Western blot images and corresponding quantification of ARG-1/β-ACTIN in the control and HKUOT-S2 treated M1 and M2 macrophages derived from the M0 macrophage. HKUOT-S2 = 0.1 μg/ml, HKUOT-P1 = 5 μg/ml. The values were shown as mean ± SEM. *p < 0.05, **p < 0.01.

analysis revealed that HKUOT-S2 treatments significantly enriched gene ontology (GO) terms associated with differentiation, development, and functions of macrophages, stem cells, and osteoblasts as well as bone formation (Fig. 6A and B). HKUOT-S2 treatments also significantly enriched the mTOR signaling pathway (Fig. 6C). These results suggest that HKUOT-S2 treatments might have modulated key osteogenic cellular components and mTOR signaling pathway to facilitate bone defect healing.

3.9. HKUOT-S2 treatment activated mTOR signaling to promote bone defect repairs

The mTOR signaling is crucial in bone development [25]. In this study, Western blot analysis revealed that the optimal dose of 2.18 mg/kg HKUOT-S2 treatment significantly activated the mTOR and 4E-BP1 proteins in the bone tissue at day 7 post-surgery (Fig. 7A–C). The qPCR results also showed that 2.18 mg/kg HKUOT-S2 treatment significantly increased the *mTOR* expression in the bone defect tissues

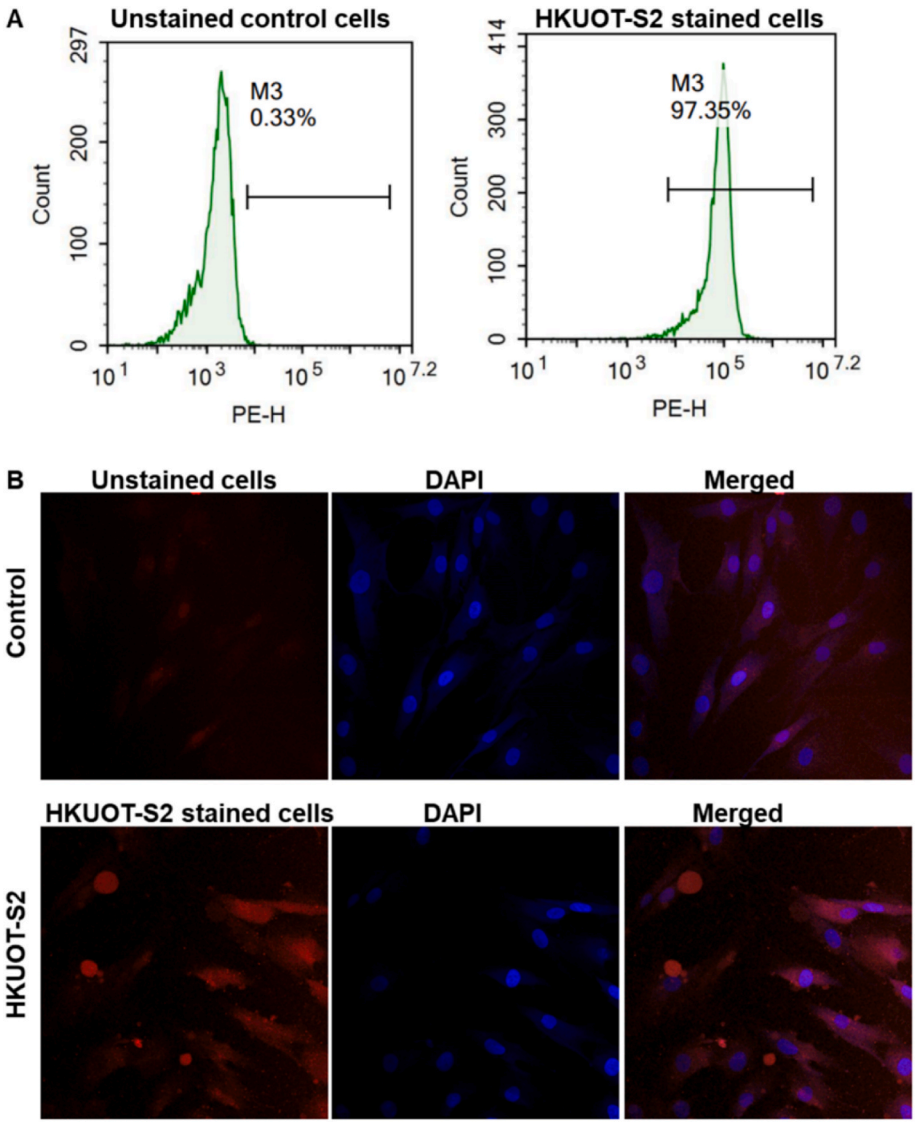

Fig. 10. HKUOT-S entered and localized in the cytoplasm of the hMSCs. A) Flow cytometry analysis showing positively stained hMSCs with Alexa Fluor 568 conjugated HKUOT-S2 protein. B) Confocal fluorescence microscope analysis showing the localization of Alexa Fluor 568 conjugated HKUOT-S2 protein in the cytoplasm and nuclei of the hMSCs.

(Fig. 7D). These results indicated that HKUOT-S2 protein treatment activated the mTOR signaling *in vivo* to promote bone defect healing.

3.10. HKUOT-S2 protein enhanced anti-inflammatory activities to promote bone defect repairs

Both pro-inflammatory and anti-inflammatory cascades play crucial roles in bone defect repairs. Moderate pro-inflammatory activities by M1 macrophages followed by anti-inflammatory activities by M2 macrophages have been reported to promote osteogenesis [54]. To evaluate whether HKUOT-S2 treatment modulated macrophage activities during the early bone defect healing process, RNAs were isolated from the bone defect sites of the sham control and the 2.18 mg/kg HKUOT-S2 treated mice at day 3 post-surgery. The qPCR analysis of RNAs extracted from the bone tissues revealed that 2.18 mg/kg HKUOT-S2 treatment induced moderate pro-inflammatory activities on day 3 post-surgery (Fig. 8A–C). HKUOT-S2 treatment, however, significantly induced anti-inflammatory activities on day 3 post-surgery to promote bone defect repairs (Fig. 8D–F). This research finding was supported by the report that M2 macrophage-induced anti-inflammatory activities could enhance osteogenesis [15]. The HKUOT-S2 protein treatment, therefore, promoted anti-inflammatory activities to facilitate bone defect healing.

3.11. HKUOT-S2 modulated M1 and M2 macrophage polarizations

It is known that M1 macrophage activities modulate bone resorption whereas M2 macrophage function facilitates new bone formation during the bone defect healing process [55]. Consequently, there are advocates for developing biomaterials with dual functions that can sequentially activate M1 and M2 macrophage activities during the bone defect-repairing process [56]. It has been reported that 50 μg/ml and 1500 μg/ml BMP2-treatment could respectively promote M1 and M2 macrophage polarization [57]. To test if the HKUOT-S2 protein also has the dual potential to polarize M1 and M2 macrophages as that of the reported BMP-2 protein, RAW264.7 cells were polarized into M1 or M2 macrophages with or without 0.1 μg/ml HKUOT-S2 protein. The qPCR results showed that HKUOT-S2 treatment could enhance both M1 and M2 macrophage polarization (Fig. 9A–D). Furthermore, it was also reported that osteogenic proteins such as BPM-2 have the potential to induce the transition from M1 to M2 macrophage phenotype to promote osteogenesis [11]. To determine whether HKUOT-S2 treatment could also switch M1 to M2 macrophage phenotype, primary

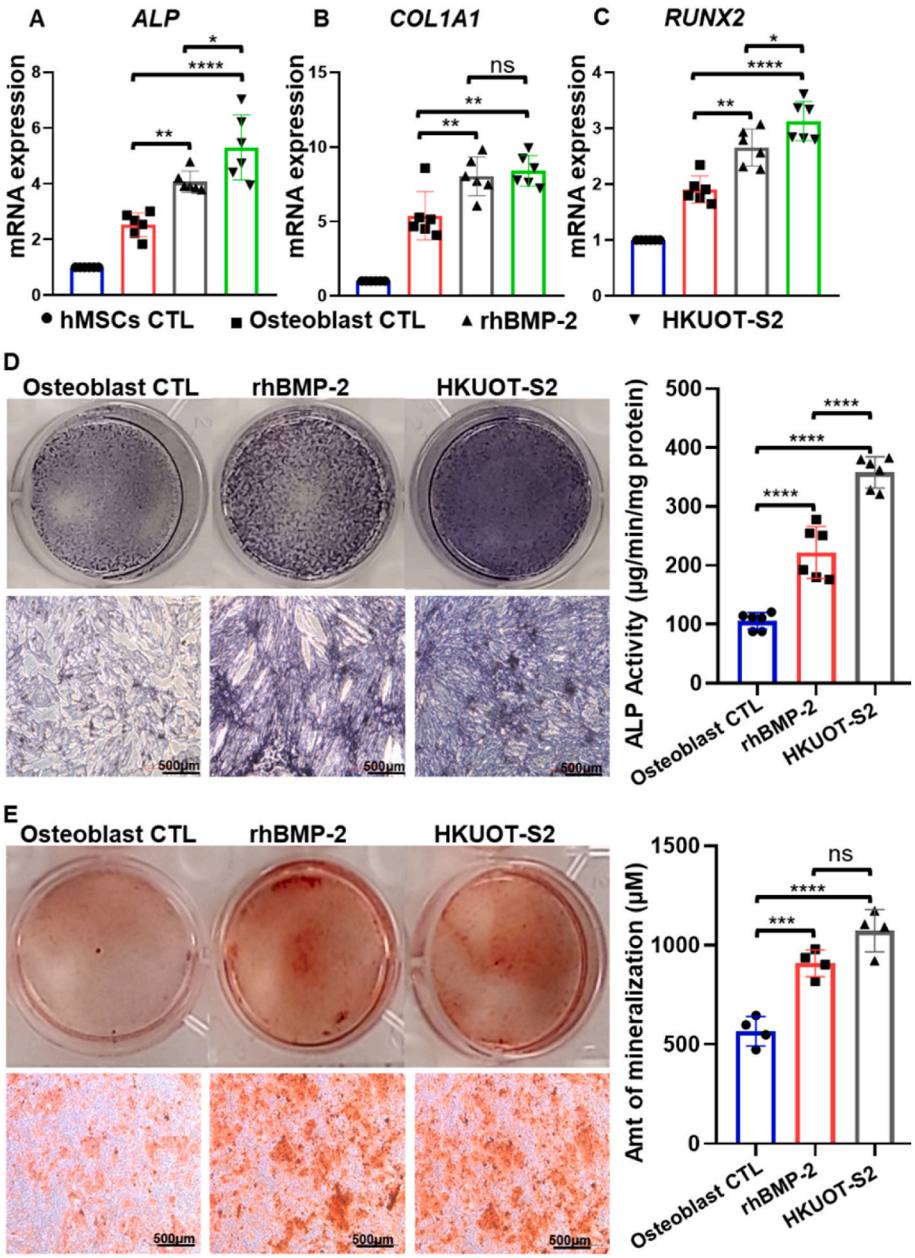

Fig. 11. HKUOT-S2 treatment enhanced hMSCs to osteoblast differentiation. A-C) Relative expression of osteogenic markers, *ALP, COL1A1,* and *RUNX2* in the hMSCs control, osteoblast control, rhBMP-2, and HKUOT-S2 treatment groups. D) Images of ALP activity and its corresponding quantification in the osteoblast control, rhBMP-2, and HKUOT-S2 treatment groups. E) Images of Alizarin Red staining of mineralized osteoblasts and its corresponding quantification in the osteoblast control, rhBMP-2, and HKUOT-S2 treatment groups.

monocytes-derived M1 and M2 macrophages with or without HKUOT-S2 treatments were co-stained with CD206 and MGL-1 antibodies. Flow cytometry analysis showed that HKUOT-S2 treatment increased CD206+ M1 macrophages compared to that of the M1 macrophage positive control. HKUOT-S2 also increased CD206, and MGL-1 double-positive M2 macrophages compared to that of the M2 positive control (Fig. 9E). Western blot analysis showed that HKUOT-S2 treatment increased the M2 macrophage marker, ARG-1 protein, in the M1 macrophage phenotype indicating that, the HNKUOT-S2 treatment might have switched the M1 macrophages towards the M2 macrophage phenotypes (Fig. 9F and G). These findings were supported by the report that BMP-2-treated M1 macrophages also expressed CD206 and ARG-1 to transit toward the M2 macrophage phenotype [11,57]. It could be deduced that a lower and single dose of HKUOT-S2 treatment has the potential to promote M1 and M2 macrophages as well as induce the transition from M1 to M2 macrophage phenotype. As anti-inflammatory M2 macrophage activities reportedly promoted osteogenesis [58], HKUOT-S2-induced M2 macrophages could promote osteoblast activities *in vivo*.

3.12. *HKUOT-S2 protein enters cells and localizes in the cell cytoplasm and nucleus*

To assess the interaction of the HKUOT-S2 protein and cells, hMSCs were treated with Alexa Fluor 568 conjugated HKUOT-S2 protein followed by flow cytometry and confocal fluorescence microscopy analyses. Flow cytometry analysis revealed that 97.35% of the hMSCs were positively stained with the fluorescent-labeled HKUOT-S2 protein when compared with the unstained control (Fig. 10A). The confocal fluorescence microscopy results confirmed that HKUOT-S2 protein entered and accumulated in both the cytoplasm and the nuclei of the hMSCs within 2hrs post-treatment when compared with the unstained control (Fig. 10B). The HKUOT-S2 protein could therefore interact with the hMSCs by entering and localizing in the cytoplasm and the nuclei to modulate cellular processes such as osteoblast differentiation based on the prevailing cellular microenvironment stimuli.

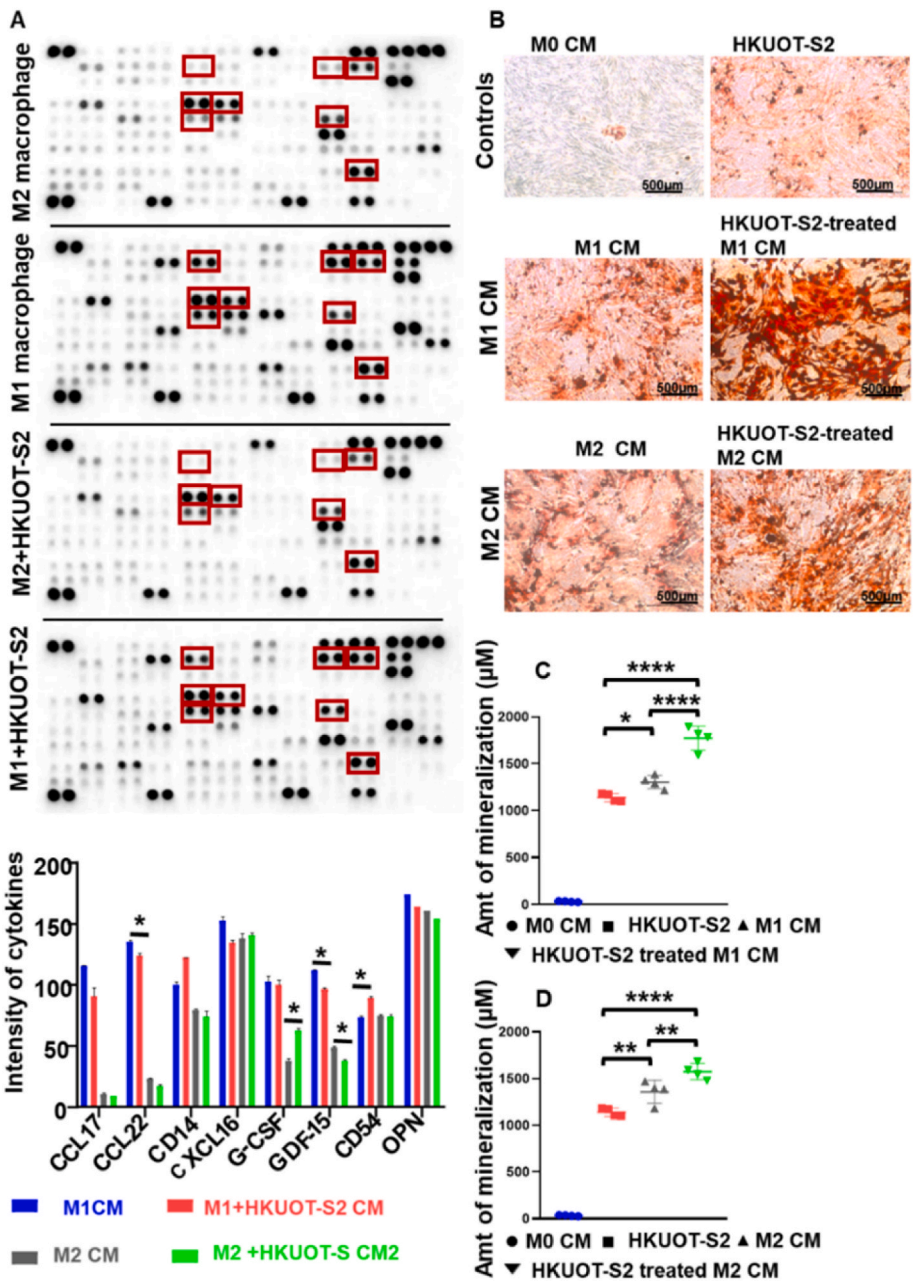

Fig. 12. HKUOT-S2 treatment enhanced the crosstalk between macrophage and MSCs to promote osteoblast biomineralization. A) Image of cytokine array analysis and its corresponding quantification in HKUOT-S2 treated M1 and M2 macrophage CM. B) Representative images of Alizarin Red staining osteoblasts treated with macrophage CM with/without HKUOT-S2 C) Quantification of Alizarin Red staining osteoblasts treated with M1 macrophage CM with/without HKUOT-S2 treatment. D) Quantification of Alizarin Red staining of osteoblasts treated with M2 macrophage CM with/without HKUOT-S2 treatment. CM = conditioned media. The values were shown as mean ± SEM, n = 5. **p < 0.01, ***p < 0.001 and ****p < 0.0001.

3.13. HKUOT-S2 treatment significantly induced osteoblast differentiation

Proteins such as BMP-2 have been known to exhibit strong osteogenic effects. It was reported that BMP-2 treatment promoted MSCs to osteoblast differentiation by significantly increasing osteoblastic ALP activity and biomineralization [59,60]. The reported dosage of 0.1 μg/ml BMP-2 treatment that induced osteogenic activity *in vitro* [59] was comparable to the 0.1 μg/ml HKUOT-S2 protein treatment that elicited osteogenic effect *in vitro*. To confirm the strength of osteogenic activities of the HKUOT-S2 protein, hMSCs were differentiated into osteoblasts with or without 0.1 μg/ml HKUOT-S2 protein and the results compared with that of the 0.1 μg/ml rhBMP2 protein as a positive control. The qPCR results showed that HKUOT-S2 protein enhanced hMSCs-osteoblast differentiation by significantly increasing *ALP* and *RUNX2* expressions (Fig. 11A, C) when compared with the BPM-2 treatment group. Although both HKUOT-S2 protein and BMP-2 treatment groups significantly increased *COL1A1* expression in the hMSCs-derived osteoblasts, there was no significant difference between the two groups (Fig. 11B). HKUOT-S2 treatment also significantly increased ALP activity in osteoblasts when compared with that of the BMP-2 treatment group (Fig. 11D). Alizarin Red staining results showed that both the HKUOT-S2 protein and BMP-2 treatment groups similarly and significantly increased osteoblast biomineralization (Fig. 11E). The *in vitro* results confirming the *in vivo* osteogenic activity of the HKUOT-S protein was supported by the report that 1.0 μg/mL dioscin from Dioscorea spp also promoted osteoblast differentiation by upregulating Alp expression [39]. It was also shown that 0.01 μg/ml HKUOT-S2 de novo peptide sequence TKSSLPGQTK could promote osteoblast differentiation by increasing ALP and COL-1A expressions *in vitro* (Figs. S7A and B). The peptide sequence TKSSLPGQTK could be a potential, functional osteogenic unit of the HKUOT-S2 protein. Recently, BMP-2 treatment has been associated with clinical adverse side effects such as ectopic bone formation, osteolysis, and stimulation of inflammation, recognized

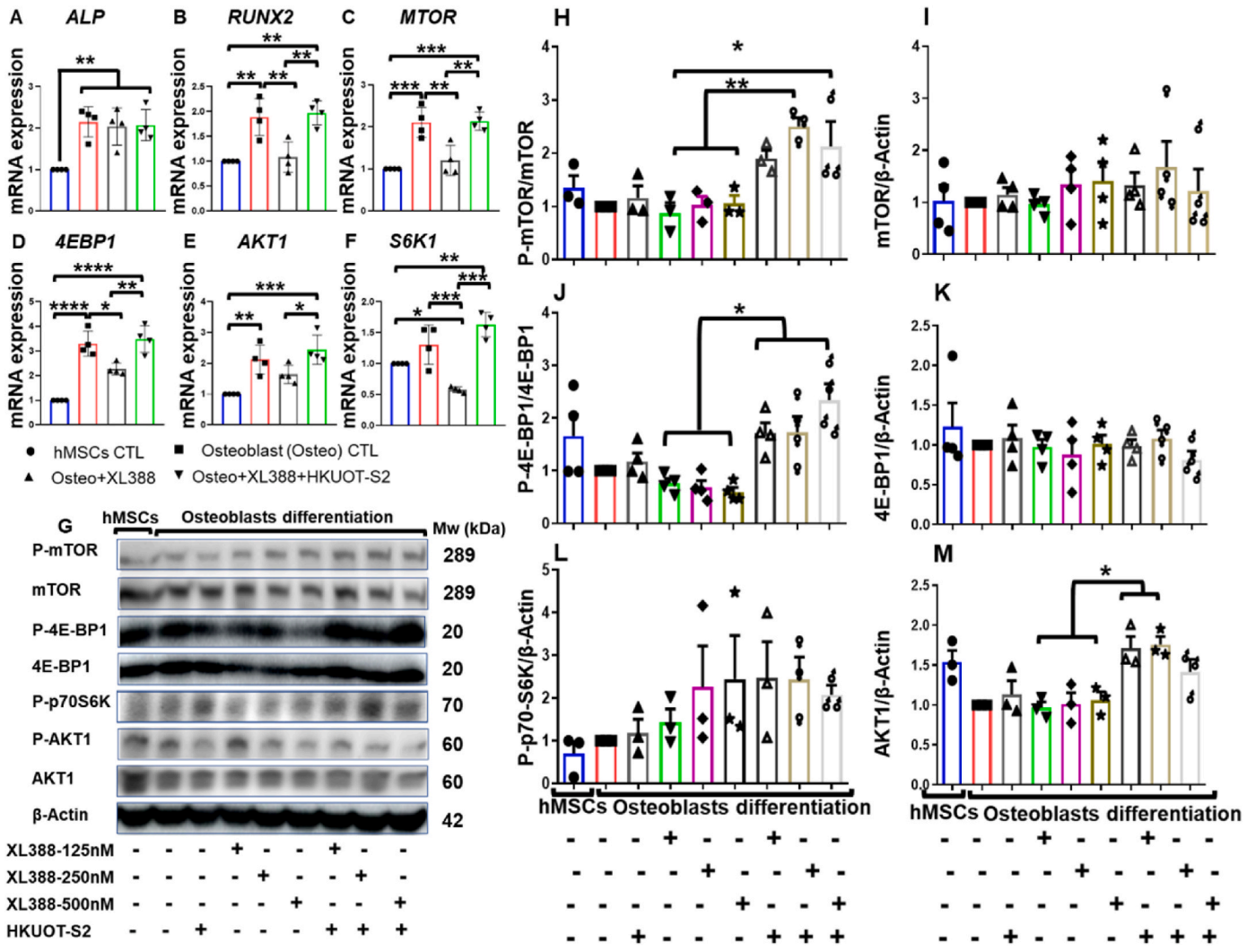

Fig. 13. HKUOT-S2 modulated mTOR/4E-BP1/S6K1/AKT1 axis to promote osteogenesis. A-F) Relative expression of *ALP, RUNX2, MTOR, 4E-BP1, AKT1,* and *S6K1* in the hMSCs control, osteoblast control, osteoblast + XL388 and osteoblast + XL388+HKUOT-S2 treatment groups. (G–M) Representative Western blot images of p-mTOR, mTOR, p-4E-BP1, 4E-BP1, P-p70S6K, p-AKT1, and AKT1 in the hMSCs control, osteoblast control, osteoblast + XL388, and osteoblast + XL388+HKUOT-S2 treatment groups. H-M) Quantification of Western blot images of p-mTOR/mTOR, mTOR/β-ACTIN, p-4E-BP1/4E-BP1 4E-BP1/β-ACTIN, P-p70S6K/β-ACTIN, and AKT1/β-ACTIN in the hMSCs control, osteoblast control, osteoblast + XL388 and osteoblast + XL388+HKUOT-S2 treatment groups. The values are shown as mean ± SEM, X-125 = 125 nM XL388. *p < 0.05, **p < 0.01, ***p < 0.001 and ****p < 0.0001.

by the FDA [12]. The HKUOT-S2 protein with stronger osteogenic activity could therefore be a potential alternative osteoanabolic agent for promoting osteogenesis and bone defect repairs.

3.14. HKUOT-S2 modulated Macrophage-MSCs crosstalk enhanced osteoblast biomineralization

Research has shown that proteins such as BMP-2 have induced macrophage-MSCs interactions to enhance osteogenesis [57]. It was reported that BMP-2 polarized macrophage condition media (CM) promoted MSCs to osteoblast differentiation *in vitro* [11]. The BMP-2-polarized macrophage CM might contain some secreted cytokines that enhanced osteoblast differentiation. To establish whether the HKUOT-S2 protein treatment could induce the secretion of osteogenic cytokines by the macrophages, U937 cells-derived macrophage CM with or without HKUOT-S2 protein treatment were subjected to cytokine array analysis. The results showed that HKUOT-S2 treatment decreased CCL17, CCL22, CXCL16, GDF-15, and OPN but increased CD14 and CD54 cytokines in the M1 macrophage CM. HKUOT-S2 treatment also increased G-CSF but decreased GDF-15 cytokines in the M2 macrophage CM (Fig. 12A). It has been reported that the M2 macrophage subtypes such as M2a and M2c moderately expressed CCL22 and highly expressed CD14 cytokines [61,62]. M2-like macrophages also reportedly expressed CD54 [63]. All these findings supported the observation that HKUOT-S2 treatment might have switched M1 to M2-like macrophage phenotypes. A study has shown that low CD14 expression impaired bone defect repairs in old rats. It was further demonstrated that $CD14^{+}$ macrophage transplantation into the bone defect sites partially rescued the impaired bone defect healing [64]. Another study has reported that the administration of G-CSF promoted bone defect healing in rats [65]. It has also been demonstrated that GDF-15 treatment promoted osteoclast differentiation but inhibited osteoblastogenesis *in vitro* [66]. In this study, the HKUOT-S2 protein reduced GDF-15 secretion in both M1 and M2 macrophage CM and that could favour osteogenesis. It was reported that modulation of various cytokines such as CD14 and CD68 favored bone regeneration in aged rats [64]. The HKUOT-S2 protein-induced secretion of cytokines (CD14, G-CSF, and GDF-15) could play critical roles in promoting osteogenesis. Moreover, the U937 cells-derived macrophage CM with or without HKUOT-S2 protein treatment was then used to differentiate hMSCs into osteoblasts. Alizarin Red S staining

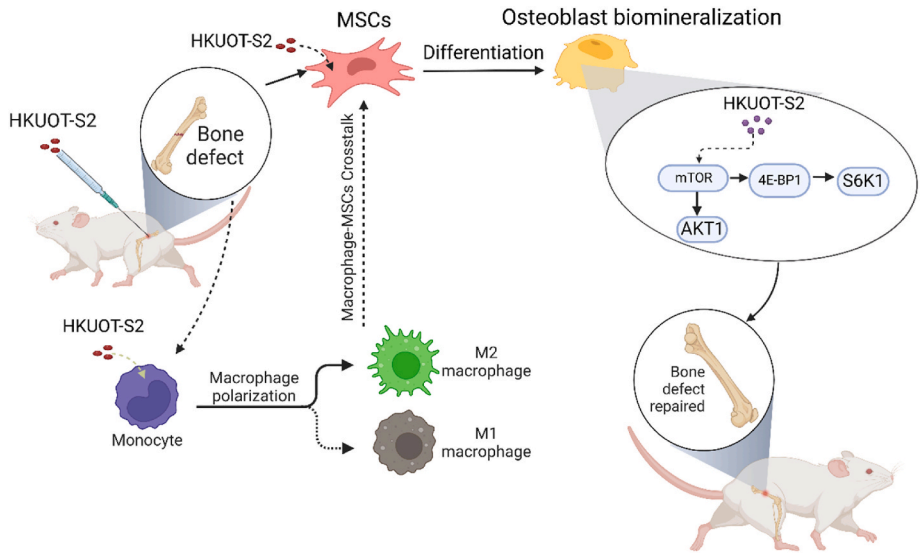

Fig. 14. Schematic diagram illustrating how HKUOT-S2 protein modulates macrophage polarization, osteoblast differentiation, and activation of the mTOR signaling axis to enhance bone defect repairs.

results showed that HKUOT-S2-treated M1 and M2 macrophage CM significantly increased osteoblast biomineralization (Fig. 12B–D), which is consistent with the reports that macrophages promoted osteogenesis [17,67]. The current finding is also supported by the report that BMP-2-treated macrophage CM also increased osteoblast biomineralization [11]. The HKUOT-S2-modulated crosstalk between macrophages and osteoblast biomineralization is further supported by the evidence that macrophage-MSCs crosstalk promoted osteoblast differentiation [16,58,64].

3.15. HKUOT-S2 activated the mTOR signaling axis to promote osteogenesis in vitro

It was reported that bone-specific mTOR knockout mice exhibited severely impaired bone development manifested by significantly decreased bone mass and osteogenic gene expressions such as *Runx2* and *Ocn* [25,68]. In this mechanistic study, inhibition of the mTOR pathway by the mTOR inhibitor (XL388) impaired osteoblast differentiation. However, HKUOT-S2 treatment restored the *RUNX2, MTORC1, 4E-BP1, AKT1, and S6K1* expressions, activated MTOR and 4E-BP1 proteins, and elevated the total AKT1 protein levels to promote the hMSCs-derived osteoblast differentiation (Fig. 13A-M). It has been reported that mTORC2 downstream target, AKT1, could indirectly activate the mTORC1 functions [69,70]. The HKUOT-S2-induced AKT1 protein expression might have also been involved in the regulation of the mTORC1 activities. Also, since the mTORC1 activity is activated by protein molecules [71], the HKUOT-S2 protein might have activated the mTORC1 and its downstream targets 4EBP1 and S6K1 to enhance osteogenesis. Taken together, it was postulated that the HKUOT-S2 protein might have modulated the mTOR signaling axis to promote osteogenesis and bone defect repairs. Clinically, the osteoanabolic HKUOT-S2 protein could be applicable in targeting the mTOR signaling pathway to facilitate bone defect healing, bone development, and general bone health.

3.16. Proposed mechanism by which HKUOT-S2 promoted bone defect healing

Based on the current research data, it was proposed that the HKUOT-S2 protein could modulate macrophage polarizations, macrophage-MSCs crosstalk, MSCs-osteoblast differentiation and activated the mTOR signaling pathway to promote bone defect repairs (Fig. 14). The HKUOT-S2 protein could be applied clinically as a potential osteogenic agent for bone defect repairs in the future.

4. Conclusion

In summary, the newly discovered HKUOT-S2 protein from *Dioscorea opposita* Thunb had no toxic effects *in vivo*. We discovered that this unique HKUOT-S2 protein could upregulate osteoblastogenesis, increase bone mineral density (BMD), modulate the crosstalk between the M1 macrophage and MSCs-derived osteoblast biomineralization, and activate the mTOR signaling axis of osteoblasts to promote osteogenesis and bone defect healing. The HKUOT-S2 protein could be a natural osteoanabolic agent for treating bone defects.

Credit author statement

John Akrofi Kubi: Conceptualization, Investigation, Methodology, Validation, Writing – original draft, Formal analysis, Writing – review & editing, Data curation, Supervision. **Augustine Suurinobah Brah**: Investigation, Methodology, Validation, Writing – original draft, Formal analysis, Writing – review & editing. **Kenneth Man Chee Cheung**: Conceptualization, Supervision, Resources, Writing – review & editing. **Yin Lau Lee**: Validation, Formal analysis, Writing – review & editing. **Kai-Fai LEE**: Validation, Formal analysis, Writing – review & editing. **Stephen Cho Wing Sze**: Validation, Writing – review & editing. **Wei Qiao**: Formal analysis, Writing – review & editing. **Kelvin Wai Kwok Yeung**: Conceptualization, Supervision, Resources, Writing – review & editing.

Ethics approval

All animal experimental procedures were carried out strictly according to the protocol approved by the University of Hong Kong (HKU) Ethics Committee, Committee on the Use of Live Animals in Teaching and Research (CULATR), (CULATR 5502–20).

Declaration of competing interest

The authors declare that they have no conflicts of interest.

Acknowledgments

This research was supported by the Seed Fund for Translational and Applied Research from the University Research Committee (URC), The University of Hong Kong (HKU), Hong Kong China (Project Codes:201910160024 and 202010160009). The authors wish to express their profound gratitude to Mr. Wong Hei Kiu (Hong Kong, China) and Mr. Shek Chun Shum (Hong Kong, China), School of Chinese Medicine, HKU, for their technical assistance during HKUOT-S2 protein purification, Mr. LIU Chi Hong Tony (Hong Kong, China) and Mr. CHAN, Chi Kwong Stephen (Hong Kong, China), Department of Orthopedics and Traumatology, HKU, for their technical assistance during μCT scan and bone tissue processing, Dr. CHEN, Andy Chun Hang, Department of Obstetrics and Gynecology, HKU, for his help in transcriptome data analysis and Centre for PanorOmics Sciences (CPOS) (Hong Kong, China), HKU, for tremendous help in mass spectrometry, de novo peptide sequencing, transcriptomic and bioinformatics analyses services.

Appendix A. Supplementary data

Supplementary data to this article can be found online at https://doi.org/10.1016/j.bioactmat.2023.04.018.

References

[1] G.B.D.F. Collaborators, Global, regional, and national burden of bone fractures in 204 countries and territories, 1990-2019: a systematic analysis from the Global Burden of Disease Study 2019, Lancet Healthy Longev 2 (9) (2021) e580–e592.
[2] C.I. Hsieh, K. Zheng, C. Lin, L. Mei, L. Lu, W. Li, F.P. Chen, Y. Wang, X. Zhou, F. Wang, G. Xie, J. Xiao, S. Miao, C.F. Kuo, Automated bone mineral density prediction and fracture risk assessment using plain radiographs via deep learning, Nat. Commun. 12 (1) (2021) 5472.
[3] L. Lafuente-Gracia, E. Borgiani, G. Nasello, L. Geris, Towards in silico models of the inflammatory response in bone fracture healing, Front. Bioeng. Biotechnol. 9 (2021), 703725.
[4] T.A. Einhorn, L.C. Gerstenfeld, Fracture healing: mechanisms and interventions, Nat. Rev. Rheumatol. 11 (1) (2015) 45–54.
[5] M. Phimphilai, Z. Zhao, H. Boules, H. Roca, R.T. Franceschi, BMP signaling is required for RUNX2-dependent induction of the osteoblast phenotype, J. Bone Miner. Res. 21 (4) (2006) 637–646.
[6] W. Huang, S. Yang, J. Shao, Y.P. Li, Signaling and transcriptional regulation in osteoblast commitment and differentiation, Front. Biosci. 12 (2007) 3068–3092.
[7] S. Maeda, M. Hayashi, S. Komiya, T. Imamura, K. Miyazono, Endogenous TGF-beta signaling suppresses maturation of osteoblastic mesenchymal cells, EMBO J. 23 (3) (2004) 552–563.
[8] C.Y. Tang, M. Wu, D. Zhao, D. Edwards, A. McVicar, Y. Luo, G. Zhu, Y. Wang, H. D. Zhou, W. Chen, Y.P. Li, Runx1 is a central regulator of osteogenesis for bone homeostasis by orchestrating BMP and WNT signaling pathways, PLoS Genet. 17 (1) (2021), e1009233.
[9] Z. Lin, D. Shen, W. Zhou, Y. Zheng, T. Kong, X. Liu, S. Wu, P.K. Chu, Y. Zhao, J. Wu, K.M.C. Cheung, K.W.K. Yeung, Regulation of extracellular bioactive cations in bone tissue microenvironment induces favorable osteoimmune conditions to accelerate in situ bone regeneration, Bioact. Mater. 6 (8) (2021) 2315–2330.
[10] H. Shen, J. Shi, Y. Zhi, X. Yang, Y. Yuan, J. Si, S.G.F. Shen, Improved BMP2-CPC-stimulated osteogenesis in vitro and in vivo via modulation of macrophage polarization, Mater Sci Eng C Mater Biol Appl 118 (2021), 111471.
[11] F. Wei, Y. Zhou, J. Wang, C. Liu, Y. Xiao, The immunomodulatory role of BMP-2 on macrophages to accelerate osteogenesis, Tissue Eng. 24 (7–8) (2018) 584–594.
[12] A.W. James, G. LaChaud, J. Shen, G. Asatrian, V. Nguyen, X. Zhang, K. Ting, C. Soo, A review of the clinical side effects of bone morphogenetic protein-2, Tissue Eng. B Rev. 22 (4) (2016) 284–297.
[13] J.R. Perez, D. Kouroupis, D.J. Li, T.M. Best, L. Kaplan, D. Correa, Tissue engineering and cell-based therapies for fractures and bone defects, Front. Bioeng. Biotechnol. 6 (2018) 105.
[14] M.T. Corvol, K. Tahiri, A. Montembault, A. Daumard, J.F. Savouret, F. Rannou, [Cell therapy in cartilage repair: cellular and molecular bases], J. Soc. Biol. 202 (4) (2008) 313–321.
[15] R.L. Shin, C.W. Lee, O.Y. Shen, H. Xu, O.K. Lee, The crosstalk between mesenchymal stem cells and macrophages in bone regeneration: a systematic review, Stem Cell. Int. (2021), 8835156, 2021.
[16] L. Gong, Y. Zhao, Y. Zhang, Z. Ruan, The macrophage polarization regulates MSC osteoblast differentiation in vitro, Ann. Clin. Lab. Sci. 46 (1) (2016) 65–71.
[17] L.Y. Lu, F. Loi, K. Nathan, T.H. Lin, J. Pajarinen, E. Gibon, A. Nabeshima, L. Cordova, E. Jamsen, Z. Yao, S.B. Goodman, Pro-inflammatory M1 macrophages promote Osteogenesis by mesenchymal stem cells via the COX-2-prostaglandin E2 pathway, J. Orthop. Res. 35 (11) (2017) 2378–2385.
[18] N. Zhang, C.W. Lo, T. Utsunomiya, M. Maruyama, E. Huang, C. Rhee, Q. Gao, Z. Yao, S.B. Goodman, PDGF-BB and IL-4 co-overexpression is a potential strategy to enhance mesenchymal stem cell-based bone regeneration, Stem Cell Res. Ther. 12 (1) (2021) 40.
[19] F. Moreno Sancho, Y. Leira, M. Orlandi, J. Buti, W.V. Giannobile, F. D'Aiuto, Cell-based therapies for alveolar bone and periodontal regeneration: concise review, Stem Cells Transl Med 8 (12) (2019) 1286–1295.
[20] S. Fitter, M.P. Matthews, S.K. Martin, J. Xie, S.S. Ooi, C.R. Walkley, J. D. Codrington, M.A. Ruegg, M.N. Hall, C.G. Proud, S. Gronthos, A.C.W. Zannettino, mTORC1 plays an important role in skeletal development by controlling preosteoblast differentiation, Mol. Cell Biol. 37 (7) (2017).
[21] X. Wei, L. Luo, J. Chen, Roles of mTOR signaling in tissue regeneration, Cells 8 (9) (2019).
[22] J. Chen, F. Long, mTORC1 signaling controls mammalian skeletal growth through stimulation of protein synthesis, Development 141 (14) (2014) 2848–2854.
[23] J. Chen, N. Holguin, Y. Shi, M.J. Silva, F. Long, mTORC2 signaling promotes skeletal growth and bone formation in mice, J. Bone Miner. Res. 30 (2) (2015) 369–378.
[24] J. Chen, F. Long, mTOR signaling in skeletal development and disease, Bone Res 6 (2018) 1.
[25] Q. Dai, Z. Xu, X. Ma, N. Niu, S. Zhou, F. Xie, L. Jiang, J. Wang, W. Zou, mTOR/Raptor signaling is critical for skeletogenesis in mice through the regulation of Runx2 expression, Cell Death Differ. 24 (11) (2017) 1886–1899.
[26] J.E. Obidiegwu, J.B. Lyons, C.A. Chilaka, The Dioscorea genus (Yam)-An appraisal of nutritional and therapeutic potentials, Foods 9 (9) (2020).
[27] S. Kim, M.Y. Shin, K.H. Son, H.Y. Sohn, J.H. Lim, J.H. Lee, I.S. Kwun, Yam (Dioscorea batatas) root and bark extracts stimulate osteoblast mineralization by increasing Ca and P accumulation and alkaline phosphatase activity, Prev Nutr Food Sci 19 (3) (2014) 194–203.
[28] K.Y. Peng, L.Y. Horng, H.C. Sung, H.C. Huang, R.T. Wu, Antiosteoporotic activity of Dioscorea alata L. Cv. Phyto through driving mesenchymal stem cells differentiation for bone formation, Evid Based Complement Alternat Med (2011), 712892, 2011.
[29] Y.W. Liu, J.C. Liu, C.Y. Huang, C.K. Wang, H.F. Shang, W.C. Hou, Effects of oral administration of yam tuber storage protein, dioscorin, to BALB/c mice for 21-days on immune responses, J. Agric. Food Chem. 57 (19) (2009) 9274–9279.
[30] K.L. Wong, Y.M. Lai, K.W. Li, K.F. Lee, T.B. Ng, H.P. Cheung, Y.B. Zhang, L. Lao, R. N. Wong, P.C. Shaw, J.H. Wong, Z.J. Zhang, J.K. Lam, W.C. Ye, S.C. Sze, A novel, stable, estradiol-stimulating, osteogenic yam protein with potential for the treatment of menopausal syndrome, Sci. Rep. 5 (2015), 10179.
[31] P. Qiu, M. Li, K. Chen, B. Fang, P. Chen, Z. Tang, X. Lin, S. Fan, Periosteal matrix-derived hydrogel promotes bone repair through an early immune regulation coupled with enhanced angio- and osteogenesis, Biomaterials 227 (2020), 119552.
[32] J.S. Kwon, S.W. Kim, D.Y. Kwon, S.H. Park, A.R. Son, J.H. Kim, M.S. Kim, In vivo osteogenic differentiation of human turbinate mesenchymal stem cells in an injectable in situ-forming hydrogel, Biomaterials 35 (20) (2014) 5337–5346.
[33] F.J. Rios, R.M. Touyz, A.C. Montezano, Isolation and differentiation of murine macrophages, Methods Mol. Biol. 1527 (2017) 297–309.
[34] B. Padhan, D. Panda, Potential of neglected and underutilized yams (Dioscorea spp.) for improving nutritional security and health benefits, Front. Pharmacol. 11 (2020) 496.
[35] S. Kumar, G. Das, H.S. Shin, J.K. Patra, Dioscorea spp. (A wild edible tuber): a study on its ethnopharmacological potential and traditional use by the local people of similipal biosphere reserve, India, Front. Pharmacol. 8 (2017) 52.
[36] N. Setyawan, J.S. Maninang, S. Suzuki, Y. Fujii, Variation in the physical and functional properties of yam (Dioscorea spp.) flour produced by different processing techniques, Foods 10 (6) (2021).
[37] R.S. Conlan, L.A. Griffiths, J.A. Napier, P.R. Shewry, S. Mantell, C. Ainsworth, Isolation and characterisation of cDNA clones representing the genes encoding the major tuber storage protein (dioscorin) of yam (Dioscorea cayenensis Lam.), Plant Mol. Biol. 28 (3) (1995) 369–380.
[38] P. Tiwwari, B. Kumar, M. Kaur, G. Kaur, H. Kaur, Phytochemical screening and extraction, A Review INTERNATIONALE PHARMACEUTICA SCIENCIA 1 (2011) 98–106.
[39] P. Hong, S. Koza, E.S. Bouvier, Size-exclusion chromatography for the analysis of protein biotherapeutics and their aggregates, J. Liq. Chromatogr. Relat. Technol. 35 (20) (2012) 2923–2950.
[40] O.T.G.f.f.o.O.G.f.C.M.o.P.O.i.H. Kong, T.P. Ip, S.K. Cheung, T.C. Cheung, T. C. Choi, S.L. Chow, Y.Y. Ho, S.Y. Kan, W.C. Kung, K.K. Lee, K.L. Leung, Y.Y. Leung, S.T. Lo, C.T. Sy, Y.W. Wong, K, Osteoporosis Society of Hong, The Osteoporosis Society of Hong Kong (OSHK): 2013 OSHK guideline for clinical management of postmenopausal osteoporosis in Hong Kong, Hong Kong Med. J. 19 (Suppl 2) (2013) 1–40.
[41] V. Tieppo Francio, S. Davani, C. Towery, T.L. Brown, Oral versus topical diclofenac sodium in the treatment of osteoarthritis, J. Pain Palliat. Care Pharmacother. 31 (2) (2017) 113–120.
[42] P. Askari, M.H. Namaei, K. Ghazvini, M. Hosseini, In vitro and in vivo toxicity and antibacterial efficacy of melittin against clinical extensively drug-resistant bacteria, BMC Pharmacol Toxicol 22 (1) (2021) 42.
[43] Y. Duan, J. Ouyang, G. Mo, W. Hao, P. Zhang, H. Yang, X. Liu, R. Wang, B. Cao, Y. Wang, H. Yu, Defensing role of novel piscidins from largemouth bass (Micropterus salmoides) with evidence of bactericidal activities and inducible expressional delineation, Microbiol. Res. 256 (2022), 126953.
[44] O. Nepal, J.P. Rao, Haemolytic effects of hypo-osmotic salt solutions on human erythrocytes, Kathmandu Univ. Med. J. 9 (34) (2011) 35–39.
[45] A. Oryan, Plant-derived compounds in treatment of leishmaniasis, Iran. J. Vet. Res. 16 (1) (2015) 1.

[46] S.J. Roberts, H.Z. Ke, Anabolic strategies to augment bone fracture healing, Curr. Osteoporos. Rep. 16 (3) (2018) 289–298.
[47] M. Girotra, M.R. Rubin, J.P. Bilezikian, Anabolic agents for osteoporosis : what is their likely place in therapy? Treat. Endocrinol. 5 (6) (2006) 347–358.
[48] S.U. Lee, S.J. Park, H.B. Kwak, J. Oh, Y.K. Min, S.H. Kim, Anabolic activity of ursolic acid in bone: stimulating osteoblast differentiation in vitro and inducing new bone formation in vivo, Pharmacol. Res. 58 (5–6) (2008) 290–296.
[49] G.E. Willick, P. Morley, J.F. Whitfield, Constrained analogs of osteogenic peptides, Curr. Med. Chem. 11 (21) (2004) 2867–2881.
[50] Z. Qian, H. Li, H. Yang, Q. Yang, Z. Lu, L. Wang, Y. Chen, X. Li, Osteocalcin attenuates oligodendrocyte differentiation and myelination via GPR37 signaling in the mouse brain, Sci. Adv. 7 (43) (2021) eabi5811.
[51] A.J. Kraus, B.G. Brink, T.N. Siegel, Efficient and specific oligo-based depletion of rRNA, Sci. Rep. 9 (1) (2019), 12281.
[52] J. Wixted, S. Challa, A. Nazarian, Enhancing fracture repair: cell-based approaches, OTA Int 5 (1 Suppl) (2022) e168.
[53] K. Nakahama, Cellular communications in bone homeostasis and repair, Cell. Mol. Life Sci. 67 (23) (2010) 4001–4009.
[54] Y.H. Wang, C.Z. Zhao, R.Y. Wang, Q.X. Du, J.Y. Liu, J. Pan, The crosstalk between macrophages and bone marrow mesenchymal stem cells in bone healing, Stem Cell Res. Ther. 13 (1) (2022) 511.
[55] W. Wang, H. Liu, T. Liu, H. Yang, F. He, Insights into the role of macrophage polarization in the pathogenesis of osteoporosis, Oxid. Med. Cell. Longev. (2022), 2485959, 2022.
[56] J.R. Alhamdi, T. Peng, I.M. Al-Naggar, K.L. Hawley, K.L. Spiller, L.T. Kuhn, Controlled M1-to-M2 transition of aged macrophages by calcium phosphate coatings, Biomaterials 196 (2019) 90–99.
[57] F. Jiang, X. Qi, X. Wu, S. Lin, J. Shi, W. Zhang, X. Jiang, Regulating macrophage-MSC interaction to optimize BMP-2-induced osteogenesis in the local microenvironment, Bioact. Mater. 25 (2023) 307–318.
[58] Y. Zhang, T. Bose, R.E. Unger, J.A. Jansen, C.J. Kirkpatrick, J. van den Beucken, Macrophage type modulates osteogenic differentiation of adipose tissue MSCs, Cell Tissue Res. 369 (2) (2017) 273–286.
[59] S.H. Kim, H.J. Choi, D.S. Yoon, C.N. Son, Serial administration of rhBMP-2 and alendronate enhances the differentiation of osteoblasts, Int J Rheum Dis 24 (10) (2021) 1266–1272.
[60] Y. Li, G. Fu, Y. Gong, B. Li, W. Li, D. Liu, X. Yang, BMP-2 promotes osteogenic differentiation of mesenchymal stem cells by enhancing mitochondrial activity, J. Musculoskelet. Neuronal Interact. 22 (1) (2022) 123–131.
[61] T. Oates, P. Moura, S. Cross, K. Roberts, H. Baum, K. Haydn-Smith, M. Wilson, K. Heesom, C. Severn, A.M. Toye, Characterizing the Polarization Continuum of Macrophage Subtypes M1, M2a and M2c, bioRxiv, 2022, 2022.06. 13.495868.
[62] A. Mantovani, A. Sica, S. Sozzani, P. Allavena, A. Vecchi, M. Locati, The chemokine system in diverse forms of macrophage activation and polarization, Trends Immunol. 25 (12) (2004) 677–686.
[63] R. Lalor, S. O'Neill, Bovine kappa-casein fragment induces hypo-responsive M2-like macrophage phenotype, Nutrients 11 (7) (2019).
[64] J. Loffler, F.A. Sass, S. Filter, A. Rose, A. Ellinghaus, G.N. Duda, A. Dienelt, Compromised bone healing in aged rats is associated with impaired M2 macrophage function, Front. Immunol. 10 (2019) 2443.
[65] F. Roseren, M. Pithioux, S. Robert, L. Balasse, B. Guillet, E. Lamy, S. Roffino, Systemic administration of G-CSF accelerates bone regeneration and modulates mobilization of progenitor cells in a rat model of distraction osteogenesis, Int. J. Mol. Sci. 22 (7) (2021).
[66] M. Westhrin, S.H. Moen, T. Holien, A.K. Mylin, L. Heickendorff, O.E. Olsen, A. Sundan, I. Turesson, P. Gimsing, A. Waage, T. Standal, Growth differentiation factor 15 (GDF15) promotes osteoclast differentiation and inhibits osteoblast differentiation and high serum GDF15 levels are associated with multiple myeloma bone disease, Haematologica 100 (12) (2015) e511–e514.
[67] R. Huang, X. Wang, Y. Zhou, Y. Xiao, RANKL-induced M1 macrophages are involved in bone formation, Bone Res 5 (2017), 17019.
[68] J. Chen, F. Long, mTORC1 signaling promotes osteoblast differentiation from preosteoblasts, PLoS One 10 (6) (2015), e0130627.
[69] H.C. Dan, A. Ebbs, M. Pasparakis, T. Van Dyke, D.S. Basseres, A.S. Baldwin, Akt-dependent activation of mTORC1 complex involves phosphorylation of mTOR (mammalian target of rapamycin) by IkappaB kinase alpha (IKKalpha), J. Biol. Chem. 289 (36) (2014) 25227–25240.
[70] A.J. Covarrubias, H.I. Aksoylar, J. Yu, N.W. Snyder, A.J. Worth, S.S. Iyer, J. Wang, I. Ben-Sahra, V. Byles, T. Polynne-Stapornkul, E.C. Espinosa, D. Lamming, B. D. Manning, Y. Zhang, I.A. Blair, T. Horng, Akt-mTORC1 signaling regulates Acly to integrate metabolic input to control of macrophage activation, Elife 5 (2016).
[71] A. Szwed, E. Kim, E. Jacinto, Regulation and metabolic functions of mTORC1 and mTORC2, Physiol. Rev. 101 (3) (2021) 1371–1426.